Article

Immunity

An Id2^{RFP}-Reporter Mouse Redefines Innate Lymphoid Cell Precursor Potentials

Highlights

- A highly sensitive *Id2*-reporter strain allows identification of ILC precursors
- Id2+ ILCPs harbor multi-potent NK and/or ILC precursors at the clonal level
- *Id2*$^{+}$*Zbtb16*$^{+}$ ILCPs retain substantial conventional NK-cell potential

Authors

Wei Xu, Dylan E. Cherrier, Sylvestre Chea, ..., Pentao Liu, Rachel Golub, James P. Di Santo

Correspondence

wei_xuxx@fudan.edu.cn (W.X.), james.di-santo@pasteur.fr (J.P.D.S.)

In Brief

Several transcription factors orchestrate innate lymphoid cell (ILC) development. By using a highly sensitive *Id2*^{RFP}-reporter mouse model, Xu et al. identify multi-potent ILC precursors that redefine branchpoints in ILC development.

Xu et al., 2019, Immunity *50*, 1054–1068
April 16, 2019
https://doi.org/10.1016/j.immuni.2019.02.022

CellPress

CellPress

Immunity
Article

An Id2^{RFP}-Reporter Mouse Redefines Innate Lymphoid Cell Precursor Potentials

Wei Xu,[1,2,3,7,*] Dylan E. Cherrier,[1,2,4,7] Sylvestre Chea,[2,5] Christian Vosshenrich,[1,2] Nicolas Serafini,[1,2] Maxime Petit,[2,4,5] Pentao Liu,[6] Rachel Golub,[2,5] and James P. Di Santo[1,2,8,*]

[1]Innate Immunity Unit, Institut Pasteur, Paris 75724, France
[2]Inserm U1223, Institut Pasteur, Paris 75724, France
[3]Department of Immunology, Shanghai Medical College, Fudan University, Shanghai 200032, China
[4]Paris Diderot University, Sorbonne Paris Cité, Paris 75013, France
[5]Lymphopoiesis Unit, Institut Pasteur, Paris 75724, France
[6]Li Ka Shing Faculty of Medicine, University of Hong Kong, Hong Kong, China
[7]These authors contributed equally
[8]Lead Contact
*Correspondence: wei_xuxx@fudan.edu.cn (W.X.), james.di-santo@pasteur.fr (J.P.D.S.)
https://doi.org/10.1016/j.immuni.2019.02.022

SUMMARY

Innate lymphoid cell (ILC) development proposes that ILC precursors (ILCPs) segregate along natural killer (NK) cell versus helper cell (ILC1, ILC2, ILC3) pathways, the latter depending on expression of *Id2*, *Zbtb16*, and *Gata3*. We have developed an *Id2*-reporter strain expressing red fluorescent protein (RFP) in the context of normal *Id2* expression to re-examine ILCP phenotype and function. We show that bone-marrow ILCPs were heterogeneous and harbored extensive NK-cell potential *in vivo* and *in vitro*. By multiplexing Id2^{RFP} with Zbtb16^{CreGFP} and Bcl11b^{tdTomato} strains, we made a single-cell dissection of the ILCP compartment. In contrast with the current model, we have demonstrated that *Id2*$^+$*Zbtb16*$^+$ ILCPs included multi-potent ILCPs that retained NK-cell potential. Late-stage ILC2P and ILC3P compartments could be defined by differential *Zbtb16* and *Bcl11b* expression. We suggest a revised model for ILC differentiation that redefines the cell-fate potential of helper-ILC-restricted *Zbtb16*$^+$ ILCPs.

INTRODUCTION

Innate lymphoid cells (ILCs) are characterized by their lack of antigen receptors and prompt reaction to signals from infected or injured tissues. Like T and B lymphocytes from the adaptive immune system, lymphocytes of the innate immune system are important players in immune responses and tolerance at mucosal barriers. ILCs have been recently re-classified into five groups (natural killer cells, NK cells; ILC1s; ILC2s; ILC3s; and lymphoid tissue inducer [LTi] cells) based on their functional outputs and expression of key transcription factors (TFs) that mirror adaptive CD8$^+$ (cluster of differentiation 8$^+$) and CD4$^+$ T cells (reviewed in Vivier et al., 2018). Although both ILC1s and conventional NK cells express T-box transcription factor (T-bet) and are capable of producing interferon-γ (IFN-γ) and tumor necrosis factor (TNF), NK cells also express Eomesodermin (Eomes) and Eomes-dependent perforin and granzymes that promote granule-dependent cytotoxic functions. ILC2s consist of cells that express the transcription factor GATA3 and are potent producers of T helper 2 (Th2)-cell-associated cytokines such as interleukin (IL)-5, IL-9, and IL-13. ILC3s are heterogeneous but uniformly express the transcription factor RORγt (RAR-related orphan receptor gamma). This group comprises CCR6$^+$CD4$^{+/-}$ and CD49a$^+$NKp46$^{+/-}$ ILC3 subsets that secrete Th17-cell-associated cytokines IL-22 or IL-17 upon activation. LTi cells are related to ILC3s but exert their function during fetal development through promotion of lymphoid-tissue organogenesis (reviewed in Cording et al., 2014).

ILCs share their developmental origins with adaptive lymphocytes (reviewed in Zook and Kee, 2016; Serafini et al., 2015). All ILC subsets are derived from common lymphoid progenitors (CLPs) in the fetal liver and adult bone marrow (BM). It is proposed that the developmental program of ILCs is similar to that of T cells, in which CLPs differentiate into specific ILC lineages by progressive loss of alternative lineage potentials. Multiple ILC-lineage-restricted progenitors downstream of CLPs have been identified. The earliest common ILC precursor (CILCP) is thought to reside in the CD135 (Flt3)$^-$α4β7$^+$ progenitor population, which still retains some T cell potential (Yu et al., 2014). The acquisition of chemokine receptor CXCR6 (C-X-C motif chemokine receptor 6) was shown to be concurrent with the loss of T cell potential in these precursors (Possot et al., 2011; Yu et al., 2014), although CXCR6 is not required for the generation of this population (Chea et al., 2015). A common helper-ILC progenitor (CHILP) has been identified using Id2^{GFP}-reporter mice (Klose et al., 2014). Id2-expressing CHILPs can give rise to all helper ILCs but fail to differentiate into killer NK cells. A distinct ILC precursor (ILCP) marked by transient expression of *Zbtb16* (encoding promyelocytic leukemia zinc finger [PLZF], a TF previously associated with NKT-cell development) has also been described (Constantinides et al., 2014). These *Zbtb16*$^+$ ILCPs fail to generate LTi and NK cells but can still generate other helper ILCs. A phase of multi-lineage priming was shown to occur in these ILCPs with co-expression of genes for different ILC lineages (Ishizuka et al., 2016). It was proposed that the final

commitment to one of the ILC lineages is influenced by external and internal signals that gradually turn off the alternative developmental programs. Despite the identification of several developmental intermediate cells along ILC-differentiation pathways, the precise stages where specific lineage programs are enabled, as well as the underlying mechanisms that restrict helper versus killer lineages, are still poorly understood (Cherrier et al., 2018; Serafini et al., 2015). This is in part due to the different model systems used (TF reporters), the varying culture conditions used to demonstrate ILCP potential, and the lack of a uniform phenotype to define ILCs that have been generated from ILCPs *in vitro* or *in vivo*.

Several TFs have been shown to be essential for early ILC differentiation, including *Nfil3*, *Tox*, *Tcf7*, and *Id2*, whose expression is initiated immediately downstream of CLPs (Ishizuka et al., 2016; Seillet et al., 2016). Loss of these factors differentially affects the generation of ILC precursors, as well as that of mature ILCs (Seehus et al., 2015; Seillet et al., 2016; Xu et al., 2015; Yang et al., 2015; Yu et al., 2014). Both *Id2* and *Tox* are required for the organogenesis of lymphoid tissues (Aliahmad et al., 2010; Yokota et al., 1999), indicating their overlapping functions in LTi-cell development during the fetal period. ID2 belongs to the family of helix-loop-helix (HLH) proteins that can form heterodimers with E proteins, thereby preventing their transcriptional activities (Kee, 2009). Inhibitor of DNA-binding (ID) proteins and E proteins play important roles in determining the cell fate in the immune system. Id2 is constitutively expressed in all ILC subsets and is indispensable for their development (Cherrier et al., 2012; Moro et al., 2010; Satoh-Takayama et al., 2010; Yokota et al., 1999). ID2 is recognized as a key regulator for establishing the ILC fate, because loss of EBF1 (early B cell factor 1), a repressor of ID2, in B cell progenitors leads to the development of ILCs and T cells (Nechanitzky et al., 2013). These findings argue for the existence of Id2-expressing lymphoid progenitors with common T and ILC potential. However, the $Id2^+$ progenitors identified using previously described Id2-reporter mice have not been shown to possess potentials for all ILC lineages and in some cases specifically lacked NK-cell potential (Jackson et al., 2011; Klose et al., 2014; Yang et al., 2011). These results contrasted with the fact that ID2 was required for normal NK-cell development (Yokota et al., 1999; Boos et al., 2007) and had been shown to be expressed in NK-committed precursors (NKPs) (Carotta et al., 2011; Rosmaraki et al., 2001), although NKPs and immature NK cells still developed in $Id2^{-/-}$ mixed-background mice, presumably due to upregulation of *Id3* expression (Boos et al., 2007). As such, $Id2^+$ CHILPs have been generally considered as a heterogeneous population that includes progenitors for ILC1s, ILC2s, and/or ILC3s, but not for conventional NK cells (reviewed in Diefenbach et al., 2014; Yang and Bhandoola, 2016).

Here, we developed an $Id2^{RFP}$-reporter mouse model and identified a complex repertoire of Id2-expressing ILC progenitors that includes common progenitors to both helper- and killer-ILC lineages. Single-cell transcriptional analysis revealed the marked heterogeneity of the ILCP population, which harbored subsets that differentially expressed *Zbtb16* and *Bcl11b*. These ILCP subsets were then further characterized using mice bearing combinations of $Id2^{RFP}$, $Zbtb16^{GFPcre}$, and $Bcl11b^{tdTomato}$ reporters. Through *in vitro* and *in vivo* assays, we could show that *Zbtb16* expression was associated with loss of ILC3 potential but not NK-cell potential, whereas *Bcl11b* expression appeared to identify an ILC2-committed progenitor, independent of *Zbtb16* expression. As such, our results redefine the cell-fate potential of putative helper-ILC-restricted $Zbtb16^+$ ILCPs as multi-potent CILCPs. In addition, TF multiplexing provides a powerful approach to identify the earliest common ILC and NK-cell progenitors as they emerge from CLPs.

RESULTS

An $Id2^{RFP}$-Reporter Strain Identifies BM NK and ILC Progenitors

To facilitate the study of Id2-expressing cells, we generated $Id2^{RFP}$-reporter mice that harbor an internal ribosome entry site monomeric red fluorescent protein (IRES-mRFP) cassette downstream of the 3′ translated region within exon 2 of the *Id2* gene ($Id2^{RFP}$) (Figure 1A). As expected, RFP was highly expressed in all ILC subsets, including splenic NK cells, liver NK cells and ILC1s, lung ILC2s, and different intestinal ILC3 subsets (Figures 1B and 1C). In contrast, RFP was poorly expressed in splenic $CD4^+$ and $CD8^+$ T cells and was not detected in B cells (Figure 1C). This pattern of RFP expression in innate and adaptive lymphocytes mirrored that of endogenous *Id2* mRNA, as shown by qRT-PCR (Figure 1D). Finally, no obvious differences in ILC development were noted in $Id2^{RFP/+}$ or $Id2^{RFP/RFP}$ mice compared with wild-type (WT) mice (data not shown). Together, these results demonstrate that $Id2^{RFP}$ mice faithfully report on *Id2* expression within major lymphocyte subsets and that the $Id2^{RFP}$ allele is functional.

A previous study of NK-cell development used an $Id2^{GFP}$ reporter in which the GFP cassette replaced one *Id2*-encoding allele (Klose et al., 2014; Rawlins et al., 2009). In this report, *Id2* was not expressed until the refined NK-cell precursor (rNKP) stage during NK-cell development, and only a small subset of the committed NK-cell progenitors expressed *Id2*. Using $Id2^{RFP}$ mice, we observed that the vast majority of rNKP cells and more than half of the pre-NKP cells expressed RFP (Figure 1E), whereas BM CLPs were Id2 negative, as shown previously (Constantinides et al., 2014; Fathman et al., 2011; Ramirez et al., 2012). These results suggest that early Id2 expression within the earliest-defined NK cells is associated with emergence of this innate lymphocyte subset from CLPs.

It was previously shown that fractions of pre-NKP and rNKP cells share phenotypic properties (*Zbtb16* and $\alpha4\beta7$ expression) with $Lin^-CD135^-\alpha4\beta7^+$ lymphoid precursors that can generate NK cells and all helper ILCs (Constantinides et al., 2015; Yu et al., 2014). We therefore examined *Id2* expression in BM ILC progenitors from $Id2^{RFP}$ mice. We found that 70% of $Lin^-CD117^+CD135^-\alpha4\beta7^+CD25^-$ BM ILCPs (which we will refer to as ILCPs) expressed RFP, whereas CLPs and the few $CD135^+\alpha4\beta7^+$ cells did not (Figure 2A; data not shown). By comparison, the subsets of relatively mature ILC2s present in BM and splenic NK cells also were clearly RFP^+ (Constantinides et al., 2014; Hoyler et al., 2012; Yu et al., 2016), although these subsets showed reduced RFP fluorescence (Figures 2A–2C).

We next made a side-by-side comparison of the previously described $Id2^{GFP}$ reporter (Klose et al., 2014; Rawlins et al., 2009) and our $Id2^{RFP}$-reporter strains. When comparing GFP and RFP expression on total BM cells, notable differences

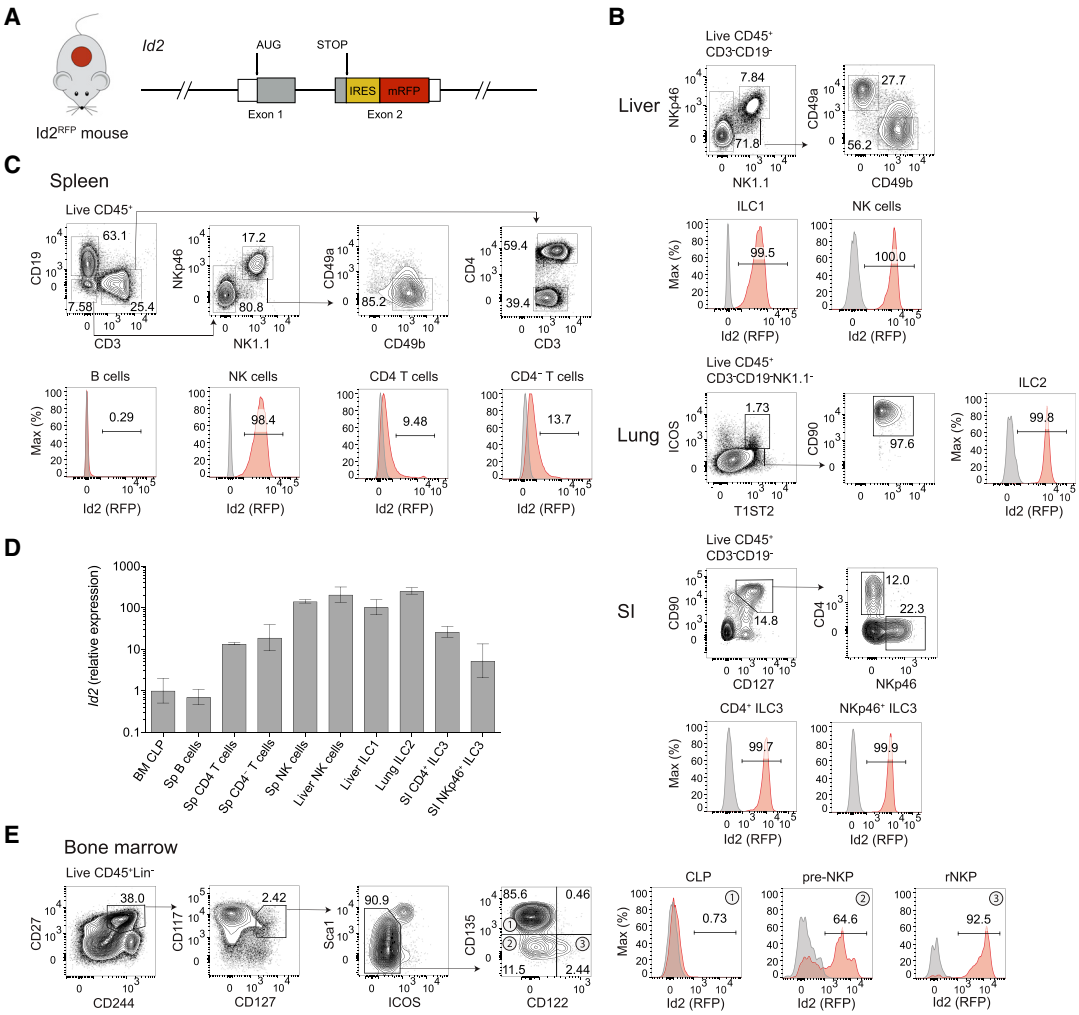

Figure 1. Characterization of *Id2*^{RFP} Reporter Mice

(A) Schematic representation of the genetic modification engineered in Id2^{RFP}-reporter mice.

(B and C) RFP expression in innate lymphoid cells isolated from (B) liver, lung and small intestine (SI), and (C) spleen of C57BL/6 (gray) and Id2^{RFP} (red) mice. Data are from one experiment representative of two independent experiments.

(D) Quantitative PCR analysis of *Id2* expression in precursor and mature cell subsets in Id2^{RFP} mice. *Id2* expression has been normalized to *Hprt* expression and to expression in CLPs. n = 3; error bars represent the standard deviation.

(E) RFP expression in BM lymphoid progenitor cells. Data are from one experiment representative of three independent experiments. Please also see Figure S1.

were observed, with the Id2^{RFP} reporter allowing detection of a larger fraction of cells with a higher mean fluorescence intensity (Figure S1A). The improved sensitivity of the Id2^{RFP} reporter over the Id2^{GFP} reporter was also apparent when comparing Id2 expression (as revealed by GFP or RFP) on gated NK cells, ILCPs, and pre-NKP cells (Figure S1B). Analysis of Id2^{GFP} × Id2^{RFP} double-reporter mice revealed that RFP^{+} cells co-expressed GFP, indicating that both reporters were active in the same cells. Together, these results indicate that our Id2^{RFP} reporter provides a highly sensitive tool to characterize *Id2*-expressing cells, including BM ILCPs.

We further compared selected cell-surface markers of Id2^{RFP} ILCPs with mature NK cells, BM CLPs, and BM ILC2s. ILCPs expressed CD244 (2B4) similarly to CLPs and NK cells, whereas KLRG1 (killer cell lectin-like receptor G1) expression was restricted to NK cells and a subset of BM ILC2s (Figure 2C). These different subpopulations showed distinct CD117 (c-Kit) and CD90 (Thy1) expression patterns (Figure 2C).

We next compared transcriptional profiles of Id2^{RFP} ILCPs to CLPs, ILC2s, and NK cells using qRT-PCR. We confirmed high amounts of *Id2* mRNA in ILCPs, ILC2Ps, and NK cells, whereas *Notch1* and *Rag2* transcripts (which are essential for B and T cell development) were very low in all subsets compared to CLPs (Figure 2D). Id2^{RFP} ILCPs expressed *Il7r* at comparable amounts to CLPs, suggesting a dependence on IL-7 signaling for ILCP emergence from lymphoid progenitors. Id2^{RFP} ILCPs expressed *Ets1*, a key transcription factor for NK and ILC2 development (Zook et al., 2016; Ramirez et al., 2012; Zook and Kee, 2016), as well as *Gata3*, which is required for the generation of ILC2s and ILC3s (Hoyler et al., 2012; Serafini et al., 2014). The

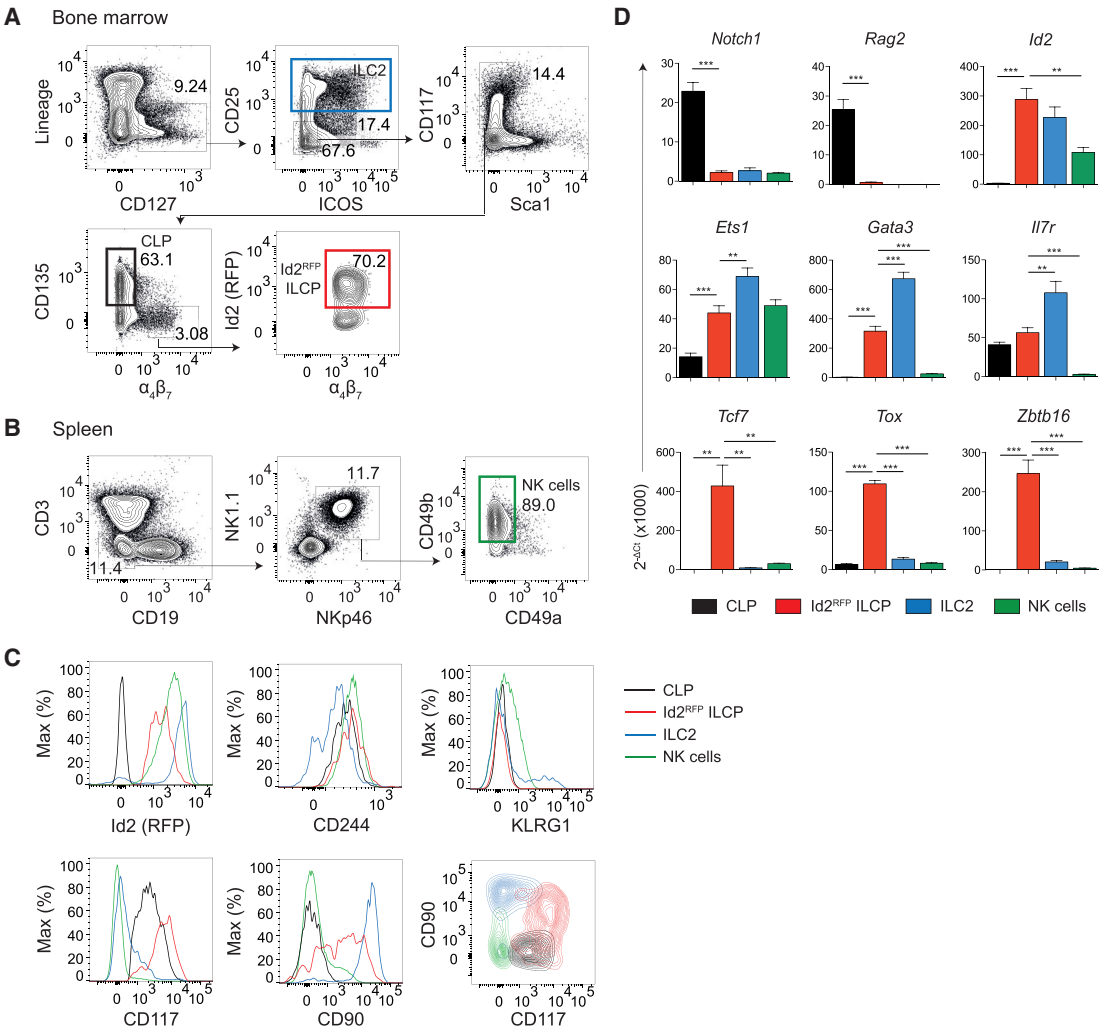

Figure 2. Characterization of *Id2*$^{+}$ BM ILCPs

(A) Flow cytometry analysis of BM ILC2s, CLPs, and ILC precursors. Data are from one experiment representative of three independent experiments.

(B) Flow cytometry analysis of splenic NK cells.

(C) Flow cytometry analysis of surface markers on CLPs, Id2^{RFP} ILCPs, ILC2s, and splenic NK cells. Data are from one experiment representative of two independent experiments.

(D) qRT-PCR analysis of TF transcripts in CLPs, Id2^{RFP} ILCPs, ILC2s, and splenic NK cells. Gene expression has been normalized to *Actb* expression. n = 6; error bars represent the standard error of the mean; *p < 0.05, **p < 0.01, ***p < 0.001, Student's t test. Please also see Figure S1.

transcription factors *Tcf7*, *Tox*, and *Zbtb16*, previously shown to mark ILC commitment (Constantinides et al., 2014; Seehus et al., 2015; Yang et al., 2015), were also highly expressed in Id2^{RFP} ILCPs but were not expressed or expressed at very low amounts in CLPs, ILC2s, or NK cells (Figure 2D). Taken together, these results validate our Id2^{RFP}-reporter mouse model that can be used to interrogate the biological properties of NK-cell progenitors and ILC progenitors, as well as mature ILC subsets in different tissues.

Id2^{+} ILCPs Harbor Common Progenitors to All ILC Lineages, Including NK Cells

In the current model of ILC development, Lin^{-}CD117^{+} CD135^{-}α4β7^{+}CD25^{-} ILCPs are considered the earliest ILC progenitors downstream of CLPs (Serafini et al., 2015; Zook and Kee, 2016), although a fraction of these cells still retain some T-cell-differentiation potential (Possot et al., 2011). As Id2 functions to block E-protein activity that is essential for T and B cell development, Id2 up-regulation is generally associated with the loss of T and B potential and the establishment of ILC fate. Our findings of Id2^{RFP} expression in a subset of BM ILCPs and in pre-NKPs (Figures 1E and 2A) led us to ask whether these subsets harbored committed progenitors for helper ILCs and/or killer NK cells and to assess their potential for other lymphoid lineages.

We first interrogated the capacity of Id2^{RFP} ILCPs to generate diverse lymphocyte subsets *in vivo*. We transferred purified CLPs or ILCPs into sub-lethally-irradiated *Rag2*$^{-/-}$*Il2rg*$^{-/-}$ recipient mice (Figure 3A). Donor-derived cells were analyzed in different organs by flow cytometry 5 weeks after transfer. As

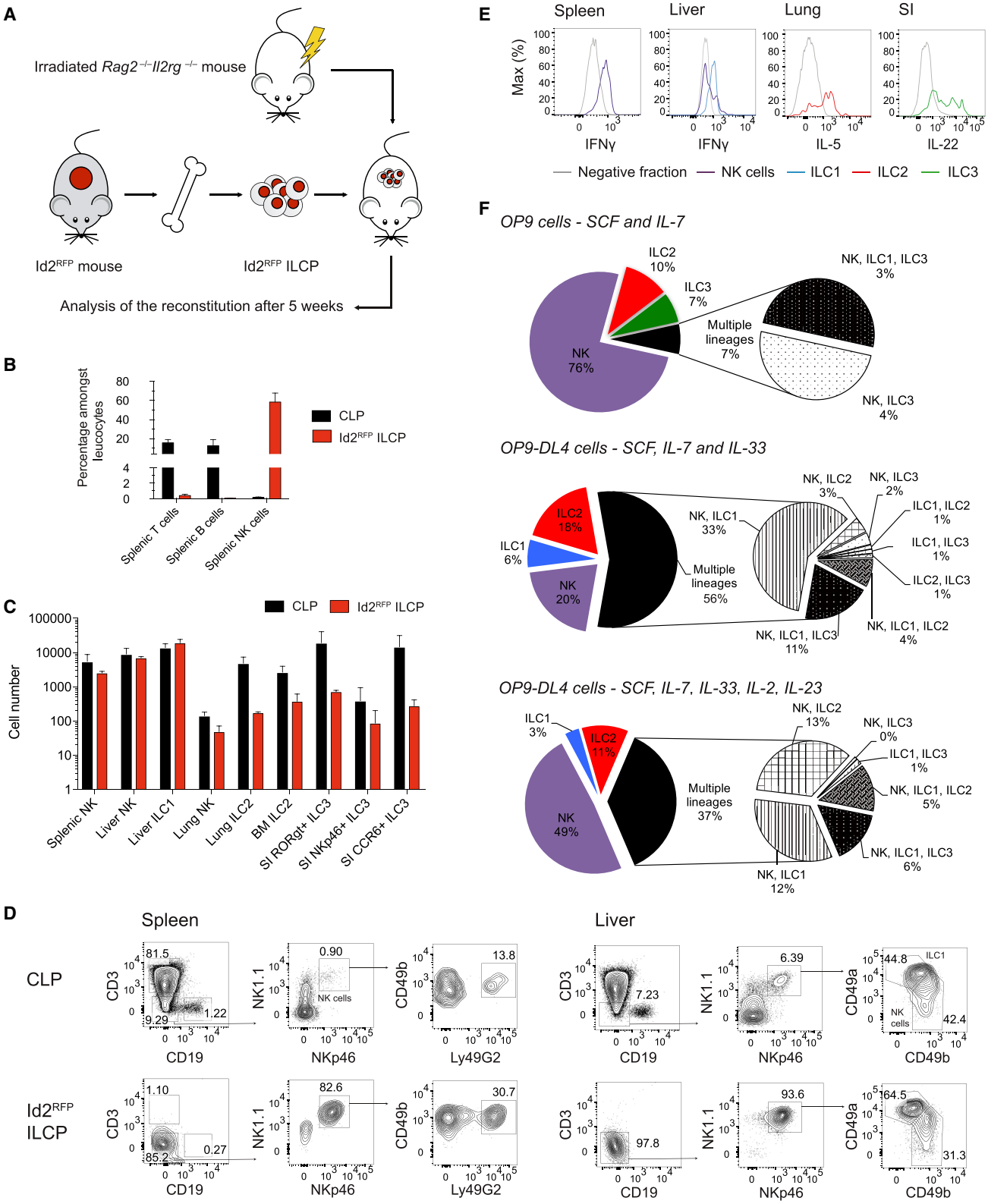

Figure 3. *Id2*$^{+}$ ILCPs Give Rise to All ILC Subsets

(A) Schematic representation of Id2^{RFP} ILCPs adoptive transfer to alymphoid *Rag2*$^{-/-}$*Il2rg*$^{-/-}$ mice.

(B and C) Reconstitution of splenic T, B, and NK cell compartments (B) and ILC compartments (C) in mice adoptively transferred with CLPs or *Id2*$^{+}$ ILCPs. n = 2–5; error bars represent standard error of the mean.

(legend continued on next page)

expected (Klose et al., 2014; Possot et al., 2011), both CLPs and Id2^{RFP} ILCPs could give rise to diverse helper-ILC subsets (including CD49a$^+$ ILC1s, ILC2s, and ILC3s; see Figure S2 for additional *in vivo* gating strategies), whereas CLPs could also give rise to T and B lymphocytes (Figures 3B and 3C). However, we also clearly detected conventional NK cells (expressing CD49b and Ly49 inhibitory receptors for major histocompatibility complex [MHC] class I) after transfer of Id2^{RFP} ILCPs (Figure 3B–3D). This result demonstrates that BM ILCPs detected using Id2^{RFP} mice harbored precursors for conventional NK cells at the population level. In contrast, such NK-cell precursors were not revealed using the Id2^{GFP}-reporter strain (Klose et al., 2014). *In-vivo*-generated NK cells and ILCs appeared functional because they were capable of producing signature cytokines after *in vitro* stimulation (Figure 3E). Our results confirm that Id2^{RFP} CD135$^-\alpha4\beta7^+$ cells harbor ILC precursors but also identify a precursor with NK-cell potential within this subset.

Generation of NK cells and ILCs *in vivo* from Id2^{RFP} ILCPs might be due to the presence of an NK-cell-committed precursor. Alternatively, a common NK-cell and ILC precursor (CILCP) that can give rise to both killer NK cells and helper ILCs could explain these findings. In order to distinguish between these possibilities, we characterized the *in vitro* lineage potential of Id2^{RFP} ILCPs. Previous reports have shown that culturing lymphoid precursors on OP9 stromal cells that do or do not express the Notch ligand Delta-like 1 could support T, NK, and helper ILC differentiation *in vitro*, depending on the cytokine milieu (Cherrier et al., 2012; Possot et al., 2011; Wong et al., 2012). Using bulk culture, we found that Id2^{RFP} ILCPs generated non-B-cell and non-T-cell populations that included not only all helper-ILC subsets but also Eomes$^+$ conventional NK cells (Figures S3A and S3B). In contrast, culture of RFP$^-$ Lin$^-$CD135$^-\alpha4\beta7^+$CD25$^-$ cells generated CD3$^+$ T cells on OP9-DL4 stroma (Figure S3A), consistent with earlier work showing that acquisition of $\alpha4\beta7$ expression by lymphoid progenitors is associated with loss of B but not T cell potential (Yoshida et al., 2001; Possot et al., 2011). Finally, *in vitro* potential from WT (non-transgenic) and Id2^{RFP} ILCPs were comparable (Figure S3C), confirming that the modified allele in Id2^{RFP} mice does not impact ILCP populations.

We further assessed the clonal heterogeneity of cell-fate potential within Id2^{RFP} ILCPs. Single ILCPs were sorted and co-cultured with OP9 or OP9-DL4 stromal cells using different cytokine combinations. The generation of various ILC subsets was assessed by flow cytometry analysis 2 weeks later. NK cells were defined as NK1.1$^+$NKp46$^+$Eomes$^+$T-bet$^+$ cells, ILC1s as NK1.1$^+$NKp46$^+$Eomes$^-$T-bet$^+$ cells, ILC2s as GATA3^{hi}CD25$^+$ ICOS$^+$ cells, and ILC3s as NKp46$^{+/-}$RORγt$^+$ cells (Figure S3B). These studies revealed several properties of Id2^{RFP} ILCPs. First, single-cell cultures of Id2^{RFP} ILCPs invariably gave rise to both single and mixed colonies of NK cells, ILC1s, ILC2s, and ILC3s (Figure 3F). This demonstrated that Id2^{RFP} ILCPs were heterogeneous and comprised multi-potent (capable of generating two or more ILC and/or NK-cell progeny) and uni-potent progenitors. Second, we found fewer colonies containing ILC2s in cultures with OP9 than in those with OP9-DL4 stromal cells (7.4% versus 28.9%), consistent with previous reports that Notch signaling is important for ILC2 generation (Wong et al., 2012). There were also more mixed-lineage ILC colonies generated in the presence of Notch ligands, suggesting that Notch signaling may be necessary to maintain or promote differentiation of multi-potent ILC precursors, as has been shown for human ILCPs (Lim et al., 2017). Third, RORγt$^+$ ILC3s were generated from Id2^{RFP} ILCPs, although these occurred at low frequency, possibly due to sub-optimal conditions for ILC3 development or expansion. Finally, a large subset of Id2^{RFP} ILCPs appeared to have robust NK-cell-lineage potential, independent of the cytokine milieu present in the cultures. These appeared mainly as uni-potent NK-cell precursors, consistent with Id2^{RFP} expression in pre-NKPs and rNKPs (Figure 1E). Nevertheless, many wells with mixed ILC lineages also harbored NK cells, indicating the presence of multi-potent Id2-expressing precursors that can give rise to both NK cells and ILCs that had not been previously appreciated (Klose et al., 2014).

Single-Cell Analysis Reveals Potential ILCP Transcriptional Trajectories

To further understand the molecular basis for the functional heterogeneity of Id2^{RFP} ILCPs, we performed single-cell transcriptional analysis by multiplex qRT-PCR. We sorted single ILCPs and CLPs from the BM of Id2^{RFP} mice and assessed the expression of 44 genes encoding TFs and surface markers that are associated with lymphoid-cell development (see Table S1). We compared these profiles with those derived from BM-resident ILC2s.

Unsupervised hierarchical clustering analysis revealed that Id2^{RFP} ILCPs had a distinct gene-expression profile compared to those of CLPs or ILC2s (Figure 4A). Four distinct clusters could be identified: cluster 1 and cluster 2 were formed by ILC2s and CLPs, respectively, whereas Id2^{RFP} ILCPs segregated into distinct clusters 3 and 4 (Figures 4A and 4B). Transcriptional signatures for cluster 2 included the cell-surface markers *CD27*, *Il7r*, and *Itga4*, as well as *Notch1*, *Rag2*, *Bcl11a*, *Runx1*, and *Ets1*, which characterize the molecular mechanisms driving CLP differentiation into the T and B cell lineages (Figure 4B). ILC-lineage-specific genes, including *Id2*, *Gata3*, *Rorc*, *Tbx21*, and *Eomes*, were not expressed in cluster 2. In contrast, cluster 1 demonstrated the expected expression signature of ILC2s, which included several TFs (*Id2*, *Rora*, *Gata3*, and *Est1*) and cell surface receptors (*Il2ra*, *Icos*, and *Il1rl1*).

Concerning Id2^{RFP} ILCPs, clusters 3 and 4 expressed the core ILC TF signature, including *Id2*, *Rora*, *Gata3*, and *Ets1*, but, unlike ILC2, also highly expressed *Tcf7*, *Tcf12*, *and Tox*. Id2^{RFP} ILCPs in clusters 3 and 4 expressed a diversity of cytokine receptors, including *Il18r1* and *Il2b* (Figure 4B), that are key drivers of NK-cell development (Hoshino et al., 1999; Suzuki et al., 1997),

(D) Spleen and liver flow cytometry analysis for ILC1s in mice adoptively transferred with CLPs or Id2^{RFP} ILCPs. Data are from one experiment representative of three independent experiments.

(E) Cytokine production of ILC subsets in mice reconstituted with Id2^{RFP} ILCPs.

(F) *In vitro* differentiation of ILCPs on OP9 or OP9-DL4 cells. Cells were cultured for 15 days with SCF and IL-7 alone or with IL-33 and/or IL-2 and IL-23. Please also see Figures S2 and S3.

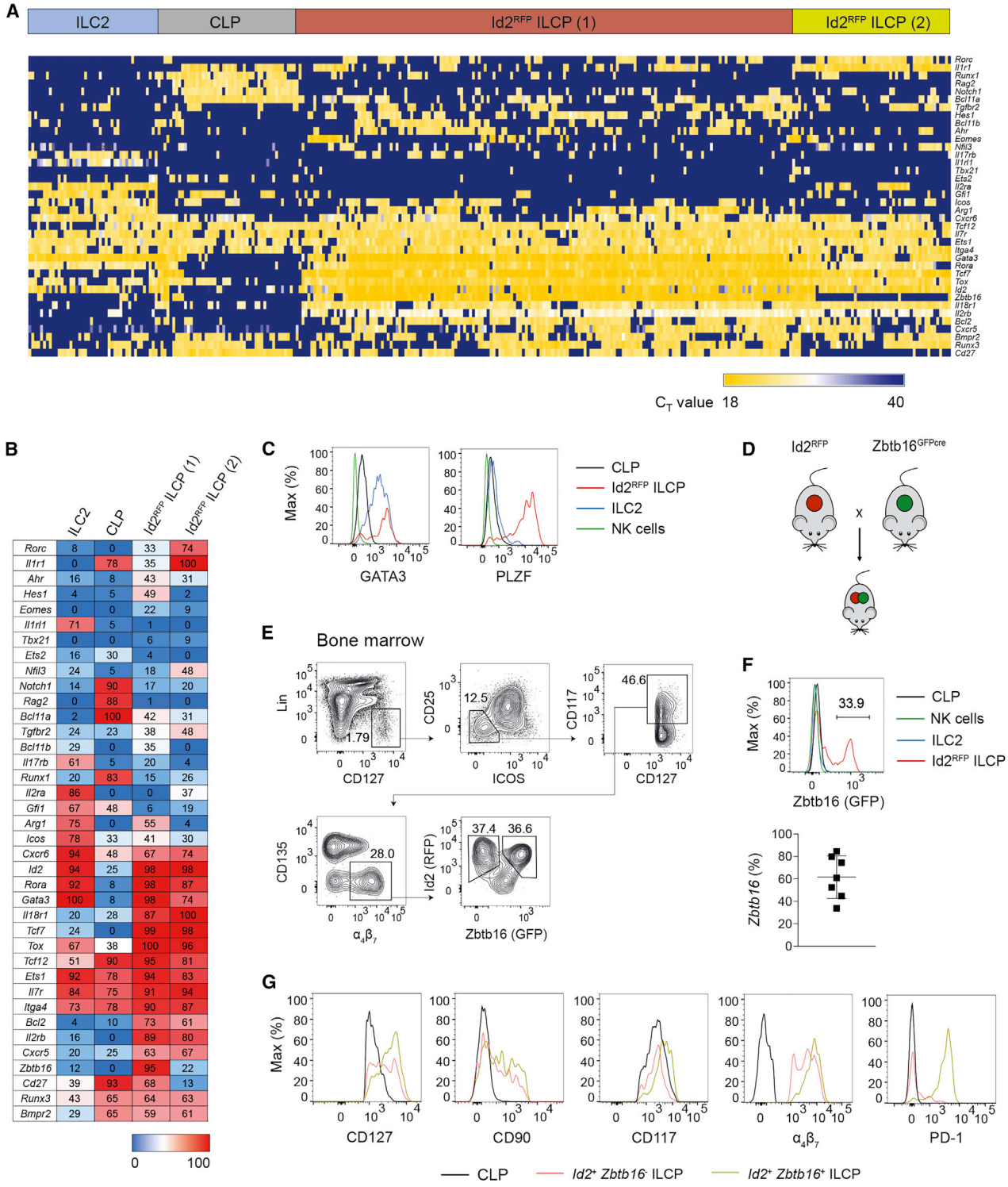

Figure 4. *Zbtb16* Expression Defines Two Subsets of *Id2*$^+$ ILCPs

(A) Single-cell multiplex qPCR ordered by hierarchical clustering of BM CLPs, *Id2*$^+$ ILCPs, and ILC2s.

(B) Percentage of single cells expressing genes of interest within CLPs, Id2^{RFP} ILCPs, and ILC2s.

(C) Fluorescence-activated cell sorting (FACS) analysis of TF expression on CLPs, *Id2*$^+$ ILCPs, ILC2s, and splenic NK cells. Data are from one experiment representative of two independent experiments.

(D) Generation of Id2^{RFP}Zbtb16^{GFPcre} double-reporter mice.

(E) Flow cytometry gating strategy for BM *Id2*$^+$*Zbtb16*$^+$ ILCPs. Data are from one experiment representative of three independent experiments.

(legend continued on next page)

although ILC1 and NK-cell transcription factors *Tbx21* and *Eomes* were mostly absent. Segregation of ILCPs in cluster 3 from those in cluster 4 was driven by the expression of *Il1r1* and *Rorc*, whereas essentially all cells in cluster 3 expressed *Zbtb16* (encoding PLZF), previously reported to identify ILCPs (Constantinides et al., 2014). Analysis of GATA3 and PLZF proteins confirmed the differential expression of these TFs in CLPs, Id2^{RFP} ILCPs, and ILC2s (Figure 4C). Taken together, the single-cell transcriptional analyses identified two closely related subsets within Id2^{RFP} ILCPs with markedly different expressions of transcription factor *Zbtb16*.

NK Lineage Potential Is Largely Retained in Id2^{+}Zbtb16^{+} ILCPs

Zbtb16-expressing cells represented about 75% of the total ILCP population in our single-cell transcriptional analysis and, as noted above, 90% of these cells expressed *Il2rb* and *Il18r1* (Figure 4B). Although a previous study showed that PLZF^{+} BM progenitors lacked NK potential (Constantinides et al., 2014), our results suggested that ILCPs expressing both Id2 and Zbtb16 might generate NK cells given the proper environmental signals. To address this hypothesis, we intercrossed Id2^{RFP} and Zbtb16^{GFPcre} strains to generate double-reporter mice (Figure 4D). Analysis of BM progenitors from Id2^{RFP}Zbtb16^{GFPcre} mice demonstrated that a fraction (ranging from 30% to 80%) of Id2^{RFP} ILCPs co-expressed Zbtb16-driven GFP (Figure 4E and 4F). The *Id2*$^{+}$*Zbtb16*$^{-}$ and *Id2*$^{+}$*Zbtb16*$^{+}$ subsets showed comparable *Id2* expression, whereas *Id2*$^{+}$*Zbtb16*$^{+}$ cells expressed higher amounts of $\alpha4\beta7$, CD117, CD127, and CD90 (Figure 4G). Moreover, we confirmed preferential expression of the inhibitory receptor PD-1 (Seillet et al., 2016; Yu et al., 2016) within the *Id2*$^{+}$*Zbtb16*$^{+}$ ILCPs (Figure 4G).

We next compared the capacity of these *Zbtb16*-expressing ILCP subsets to further differentiate *in vivo*. *Id2*$^{+}$*Zbtb16*$^{-}$ and *Id2*$^{+}$*Zbtb16*$^{+}$ ILCPs were purified from Id2^{RFP}Zbtb16^{GFPcre} mice and transferred into *Rag2*$^{-/-}$*Il2rg*$^{-/-}$ hosts. Both populations generated exclusively ILC and NK-cell progeny and lacked potential for B, T, or myeloid cells. Similar to results previously reported for *Zbtb16*$^{+}$ ILCPs (Constantinides et al., 2014), *Id2*$^{+}$ *Zbtb16*$^{+}$ ILCPs gave rise to multiple ILC lineages (ILC1, ILC2, and ILC3) in different tissues (Figure 5A). However, NK cells expressing inhibitory Ly49 receptors were clearly detected in the spleen and Eomes^{+} or CD49b^{+} NK cells were detected in the liver (Figure 5B), although CD49a^{+} ILC1s dominated in the latter, as expected (Constantinides et al., 2014). A similar pattern was observed after transfer of *Zbtb16*$^{-}$ ILCPs (Figure 5A and 5B). Taken together, these results confirm that BM *Id2*$^{+}$*Zbtb16*$^{+}$ ILCPs can give rise to ILC1s, ILC2s, and ILC3s *in vivo* (Constantinides et al., 2014) but also demonstrate that *Id2*$^{+}$*Zbtb16*$^{+}$ ILCPs retain NK-lineage potential.

We further characterized Id2^{RFP}Zbtb16^{GFPcre} progenitors using clonal assays. Single *Id2*$^{+}$*Zbtb16*$^{+}$ ILCPs were purified and cultured on OP9 or OP9-DL4 stromal cells, and the development of different ILC subsets was determined by flow cytometry as above. We found that *Id2*$^{+}$*Zbtb16*$^{+}$ ILCPs generated colonies of single or mixed ILC lineages (Figure 5C), confirming previous studies (Constantinides et al., 2014). To our surprise, many single-cell cultures of *Id2*$^{+}$*Zbtb16*$^{+}$ ILCPs also harbored NK cells (Figure 5C; Table S2). Nearly 80% of the wells derived from *Id2*$^{+}$ *Zbtb16*$^{+}$ ILCPs contained Eomes^{+} NK cells, which was comparable to results using unfractionated ILCPs (85.2%) (Figure 3F; Table S2). In contrast, the percentage of mixed-lineage colonies derived from *Id2*$^{+}$*Zbtb16*$^{+}$ ILCPs was lower than that obtained with total ILCPs (13.9% from *Id2*$^{+}$*Zbtb16*$^{+}$ ILCPs versus 37.1% from *Id2*$^{+}$ ILCPs), and the frequencies of colonies containing ILC1s or ILC3s were also reduced, in agreement with a more restricted lineage potential of *Id2*$^{+}$*Zbtb16*$^{+}$ ILCPs. Phenotypic analysis of the NK cells generated from *Id2*$^{+}$*Zbtb16*$^{+}$ ILCPs confirmed their cytotoxic potential (Figure 5D).

Id2, Zbtb16, and Bcl11b Transcripts Define Lineage Restriction of ILC Progenitors

To better understand the relationship between *Id2*$^{+}$*Zbtb16*$^{-}$ and *Id2*$^{+}$*Zbtb16*$^{+}$ ILCP subsets, we performed multiplex qRT-PCR for gene-expression analysis of the two populations. Single CLPs, *Id2*$^{+}$*Zbtb16*$^{-}$ and *Id2*$^{+}$*Zbtb16*$^{+}$ ILCPs were purified from Id2^{RFP}Zbtb16^{GFPcre} BM and 44 lymphoid genes were examined as described above. Using unsupervised hierarchical clustering, we found that *Id2*$^{+}$*Zbtb16*$^{+}$ ILCPs and *Id2*$^{+}$*Zbtb16*$^{-}$ cells were closely related but could be distinguished (Figure 6A). As expected, the expression of *Zbtb16* was restricted to *Id2*$^{+}$*Zbtb16*$^{+}$ ILCPs. The expression of several ILC-related genes, including *Id2*, *Tox*, *Tcf7*, *Gata3*, and *Rora*, gradually increased from *Id2*$^{+}$ *Zbtb16*$^{-}$ to *Id2*$^{+}$*Zbtb16*$^{+}$ ILCPs. These results implied a close developmental relationship between the *Id2*$^{+}$*Zbtb16*$^{-}$ and *Id2*$^{+}$ *Zbtb16*$^{+}$ ILCPs. Accordingly, short-term culture of *Id2*$^{+}$*Zbtb16*$^{-}$ ILCPs generated a discrete subset of *Zbtb16*$^{+}$ cells (Figure 6B) consistent with previous studies (Constantinides et al., 2014).

In addition to *Zbtb16*, we identified several genes that were enriched in *Id2*$^{+}$*Zbtb16*$^{+}$ ILCPs, including *Bcl11b*, a TF essential for ILC2 development (Califano et al., 2015; Yu et al., 2015); *Arg1*, a urea cycle enzyme that marks ILC precursors in the fetal gut and plays a key role in regulating ILC2 functions (Bando et al., 2015; Monticelli et al., 2016); and *Hes1*, a downstream target of Notch signaling (Ohtsuka et al., 1999). Conversely, we found that *Rorc*, a pivotal transcription factor for the generation of ILC3 lineages, as well as *Il1r1* and *Il2ra*, receptor subunits required for IL-1β and IL-2 signaling, respectively, were preferentially expressed in *Id2*$^{+}$*Zbtb16*$^{-}$ ILCPs.

The reduced frequency of *Rorc* and *Il1r1* transcripts in the *Id2*$^{+}$*Zbtb16*$^{+}$ ILCPs led us to speculate that these cells may have lower ILC3-lineage potential than *Id2*$^{+}$*Zbtb16*$^{-}$ ILCPs. To test this possibility, we cultured *Id2*$^{+}$*Zbtb16*$^{-}$ and *Id2*$^{+}$*Zbtb16*$^{+}$ ILCPs on OP9 or OP9-DL4 stromal cells and compared their differentiation capacity *in vitro*. Indeed, few ILC3s were generated from *Id2*$^{+}$*Zbtb16*$^{+}$ ILCPs, whereas RORγt^{+} ILC3s were detected

(F) GFP expression in CLPs, Id2^{RFP} ILCPs, ILC2s, and splenic NK cells of Id2^{RFP}Zbtb16^{GFPcre} mice (top) and percentage of Zbtb16^{GFP} expression in *Id2*$^{+}$ ILCPs (n = 7) (bottom).

(G) Flow cytometry analysis of surface marker expression on CLPs and *Id2*$^{+}$*Zbtb16*$^{-}$ and *Id2*$^{+}$*Zbtb16*$^{+}$ ILCPs. Data are from one experiment representative of two independent experiments.

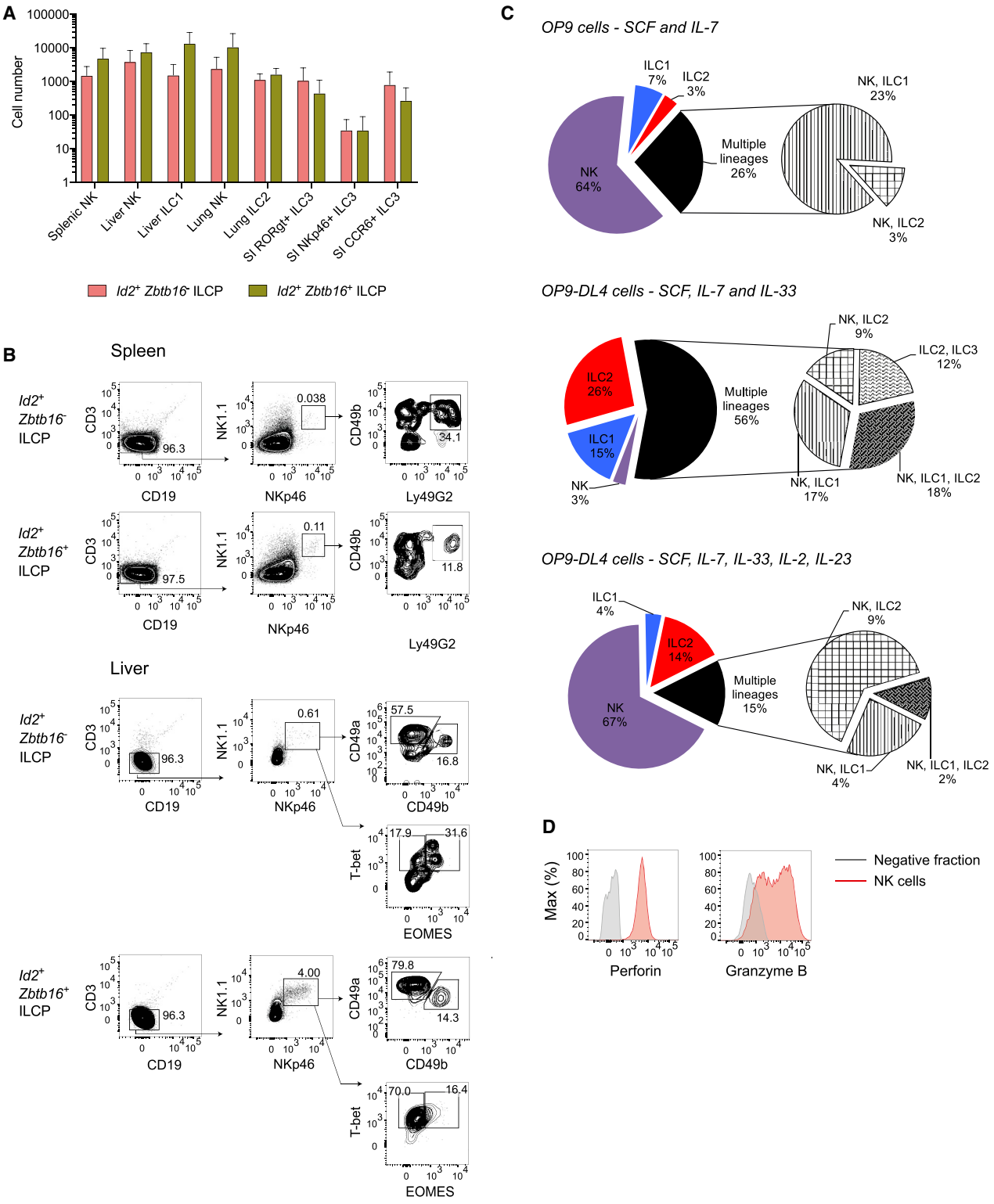

Figure 5. *Id2*$^{+}$*Zbtb16*$^{+}$ ILCPs Retain NK-Cell Potential

(A) Reconstitution of ILC compartments in mice adoptively transferred with *Id2*$^{+}$*Zbtb16*$^{-}$ or *Id2*$^{+}$*Zbtb16*$^{+}$ ILCPs (n = 4; error bars represent standard error of the mean).

(B) Spleen and liver FACS analysis for ILC1s in mice adoptively transferred with *Id2*$^{+}$*Zbtb16*$^{-}$ or *Id2*$^{+}$*Zbtb16*$^{+}$ ILCPs. Data are from one experiment representative of two independent experiments.

(legend continued on next page)

in cultures derived from *Id2*$^{+}$*Zbtb16*$^{-}$ ILCPs (Figure 6C) with little effect of enforced Notch signaling. These RORγt^{+} ILC3s also expressed CCR6, a chemokine receptor expressed by LTi cells, and were NKp46^{-} (Figure 6C). Together, these data demonstrated that *Zbtb16* expression in ILC precursors is associated with progressive loss of capacity to generate the ILC3 lineage, especially CCR6^{+} ILC3s.

The transcription factor *Bcl11b* was proposed as a global early ILCP marker that is further up-regulated in ILC2-restricted precursors and required for ILC2 development (Califano et al., 2015; Yu et al., 2015). Our single-cell multiplex gene-expression data revealed that *Bcl11b* is expressed in a subset of *Id2*$^{+}$ ILCPs and preferentially expressed in *Id2*$^{+}$*Zbtb16*$^{+}$ ILCPs. To further explore the function of these different *Id2*$^{+}$ ILCPs subsets, we intercrossed Bcl11b^{tdTomato} (Li et al., 2010) and Id2^{RFP}Zbtb16^{GFPcre} mice to generate Id2^{RFP}Zbtb16^{GFPcre} Bcl11b^{tdTomato} triple-reporter mice. Analysis of the BM progenitor cells from these mice showed that *Zbtb16* and *Bcl11b* expression divided Id2^{RFP} ILCPs into four discrete subsets: *Zbtb16*$^{-}$*Bcl11b*$^{-}$, *Zbtb16*$^{+}$*Bcl11b*$^{-}$, *Zbtb16*$^{+}$*Bcl11b*$^{+}$, and *Zbtb16*$^{-}$*Bcl11b*$^{+}$ ILCPs (Figure 7A).

We next compared the expression of several cell-surface markers of BM progenitors or ILC2s among these four subsets. Although all comparably expressed CD27, CD117, and CD90 (Figure 7B), PD-1 was strictly expressed by *Zbtb16*$^{+}$ ILCPs regardless of *Bcl11b* expression, and none of the subsets expressed CD25, which characterizes late-stage ILC2 differentiation. A fraction of *Zbtb16*$^{-}$*Bcl11b*$^{-}$ ILCPs expressed RORγt and lower amounts of CD27 compared to other subsets (Figure 7C), in accordance with the transcriptional profile of *Id2*$^{+}$*Zbtb16*$^{-}$ ILCPs (Figure 6A). To compare the developmental potential of these four Id2^{RFP} ILCPs subsets, we bulk cultured purified *Zbtb16*$^{-}$*Bcl11b*$^{-}$, *Zbtb16*$^{+}$*Bcl11b*$^{-}$, *Zbtb16*$^{+}$*Bcl11b*$^{+}$, and *Zbtb16*$^{-}$*Bcl11b*$^{+}$ ILCPs on OP9-DL4 stromal cells with cytokines and characterized their progeny. *Bcl11b*-expressing ILCPs, regardless of *Zbtb16* expression, grew poorly in IL-7 and stem cell factor (SCF) (Figure S3D). When IL-33 was added to the cultures, robust ILC2 growth was observed (Figures 7D and 7E), indicating that these cells were highly enriched in ILC2 precursors, consistent with previous reports (Califano et al., 2015; Yu et al., 2015). In contrast, *Zbtb16*$^{+}$*Bcl11b*$^{-}$ ILCPs could generate NK cells, ILC1s, and ILC2s but only few ILC3s. Only *Zbtb16*$^{-}$*Bcl11b*$^{-}$ ILCPs could give rise to all three ILC lineages (ILC1, ILC2, and ILC3) as well as NK cells (Figures 7D and 7E). Clonal analyses confirmed these findings (Figure 7F). Thus, *Zbtb16*$^{-}$*Bcl11b*$^{-}$ ILCPs harbor the earliest BM Id2^{RFP} ILCPs that can generate all ILC and NK-cell lineages.

DISCUSSION

Using a highly sensitive Id2^{RFP}-reporter mouse model, we have characterized heterogeneous progenitor populations in adult BM that include ILCPs and NK-cell-restricted precursors (NKPs). These Id2^{RFP} ILCPs are comprised of both multi-potent (giving rise to multiple ILC lineages, including conventional NK cells) and uni-potent precursors, with potential for a single ILC group or for conventional NK cells. By multiplexing our Id2^{RFP} reporter with existing TF reporters (Zbtb16^{GFPcre} and Bcl11b^{tdTomato}), we could simultaneously assess the impact of three key transcription factors (*Id2*, *Zbtb16*, and *Bcl11b*) to ILC development and uncover the substantial phenotypic and functional heterogeneity of Id2^{RFP} ILCPs. Through single-cell qPCR analysis and *in vitro* clonal assays, we could redefine the earliest common ILCPs downstream of the common lymphoid progenitor and clarify the contribution of several TFs at the different stages of ILC development. Based on these results, we propose a revised scheme of murine BM ILC and NK-cell differentiation that markedly contrasts with the current helper versus killer model (Figure S4).

The Id2^{RFP} reporter used in this study provided a key tool to dissect ILCP diversity due to robust and distinct fluorescence properties. Compared with the previously described Id2^{GFP} mice used to identify CHILPs (Klose et al. 2014), our Id2^{RFP} reporter has brighter fluorescence, which allowed for the identification of a larger fraction of *Id2*-expressing cells in the BM. Because RFP can be spectrally separated from GFP, YFP, and tdTomato fluorochromes using standard flow cytometers, we could take advantage of multiplexed fluorescent reporters to isolate distinct ILCP subpopulations that differentially expressed three key transcription factors required for ILC development. This allowed us to perform an in-depth phenotypic, transcriptomic, and functional analysis of Id2^{RFP} ILCP subsets both *in vivo* and *in vitro*. Importantly, we used standardized and widely accepted criteria for identifying mature ILC subsets derived from these different ILCPs. This was a critical issue because previous reports have not always used the same defining markers for NK cells and ILC progeny of ILCPs (Constantinides et al., 2014; Klose et al., 2014), leading to some question about the precursor-product relationship of ILCPs with mature ILC and NK cells.

Based on studies using Id2^{GFP} mice, Klose et al. (2014) identified an ILCP population (CHILPs) that could give rise *in vitro* and *in vivo* to several ILC subsets (Eomes^{-} ILC1, ILC2, and ILC3) but not to conventional Eomes^{+} NK cells. The authors proposed a killer versus helper model of ILC and NK-cell development from CLPs in which NK cells emerge prior to the *Id2*$^{+}$ CHILP stage, although other ILC subsets are CHILP derived. The authors also suggested that early NK-cell development was relatively Id2 independent because only low amounts of GFP were detected in NKPs from *Id2*^{GFP} mice (Klose et al., 2014). In contrast, we have provided evidence for *Id2*-expressing lymphoid progenitors in Id2^{RFP} mice with potential for all ILC lineages, including NK cells. These differences may be explained by the better discrimination of these rare cells in Id2^{RFP} mice, allowing for isolation of multi-potent ILCPs and NKPs. Single-cell assays demonstrate that ILCPs can generate both conventional

(C) *In vitro* differentiation of *Id2*$^{+}$*Zbtb16*$^{+}$ ILCPs on OP9 or OP9-DL4 cells. Cells were cultured during 15 days with SCF and IL-7 or with IL-33 and/or IL-2 and IL-23. (D) Analysis of perforin and granzyme B expression in NK cells derived from bulk culture of 200 *Id2*$^{+}$*Zbtb16*$^{+}$ ILCPs. Cells were cultured during 7 days on OP9 cells with SCF and IL-7 and supplemented for 1 day with IL-12 and IL-15. Data are from one experiment representative of two independent experiments, each including technical triplicates.

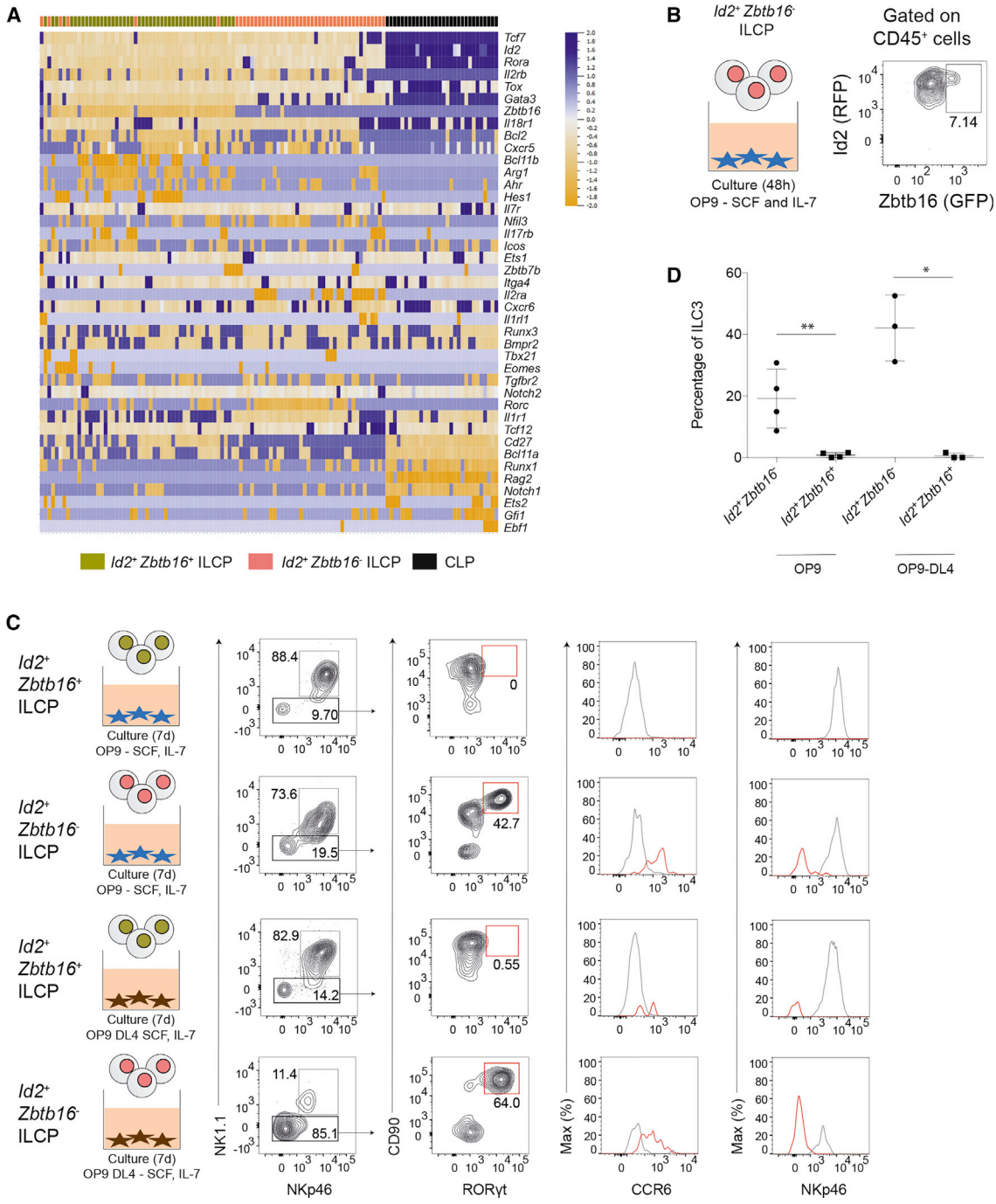

Figure 6. *Id2*$^+$*Zbtb16*$^+$ ILCPs Derive from *Id2*$^+$*Zbtb16*$^-$ Cells with Loss of ILC3 Potential

(A) Single-cell multiplex qPCR ordered by hierarchical clustering of BM CLPs and *Id2*$^+$*Zbtb16*$^-$ and *Id2*$^+$*Zbtb16*$^+$ ILCPs.

(B) RFP and GFP expression on *Id2*$^+$*Zbtb16*$^-$ ILCPs cultured for 48 h on OP9 cells with SCF and IL-7. Data are from one experiment representative of three independent experiments.

(C) Flow cytometry analysis for ILC3s after culture of *Id2*$^+$*Zbtb16*$^-$ ILCPs and *Id2*$^+$*Zbtb16*$^+$ ILCPs or 7 days on OP9 or OP9-DL4 cells with SCF and IL-7. Data are from one experiment representative of two independent experiments, each including technical duplicates.

(D) Percentage of ILC3s among CD45$^+$ cells after 7 days' culture of *Id2*$^+$*Zbtb16*$^-$ and *Id2*$^+$*Zbtb16*$^+$ ILCPs on OP9 or OP9-DL4 cells with SCF and IL-7. n = 3 or 4; error bars represent standard error of the mean; *p < 0.1, **p < 0.05, Mann-Whitney U test.

Eomes$^+$ NK cells and different ILC subsets, providing evidence for a common ILC and NK-cell progenitor that expresses *Id2*. Our results argue against the notion of separate "branches" of killer-NK-cell and helper-ILC development that are *Id2* independent and *Id2* dependent, respectively. Rather, we envisage a model of *Id2*-mediated suppression of adaptive B and T cell

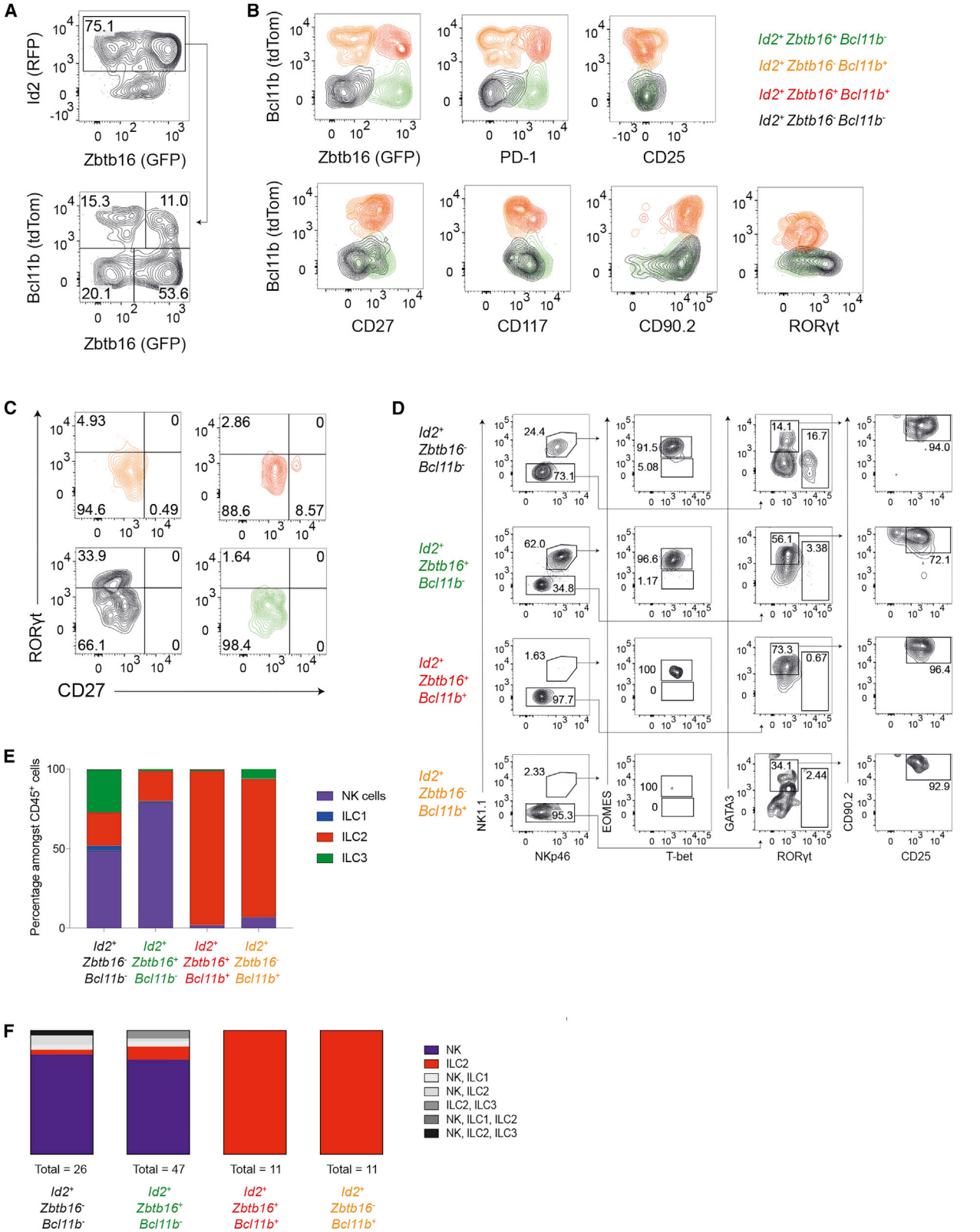

Figure 7. *Bcl11b* Marks Emergence of an ILC2-Restricted Precursor

(A) Flow cytometry characterization of Lin$^-$CD127$^+$CD25$^-$ICOS$^-$CD117$^+$CD135$^-$$\alpha_4\beta_7^+$ cells from Id2^{RFP}Zbtb16^{GFPcre}Bcl11b^{tdTomato} mice.

(B) Flow cytometry analysis of surface marker and transcription factor expression on Id2^{RFP} ILCPs according to their expression of *Zbtb16* and *Bcl11b*.

(legend continued on next page)

development from CLPs that is associated with emergence of CILCPs and NK-cell precursors (Figure S4). This revised model places committed NK-cell progenitors (Fathman et al. 2011; Rosmaraki et al., 2001) downstream of CILCPs.

Previous studies using Zbtb16^{GFPCre} reporter mice identify a PLZF$^+$ ILCP (Constantinides et al., 2014) that shows a phenotypic and functional overlap with *Id2*$^+$ CHILPs (Klose et al., 2014). *Zbtb16*$^+$ ILCPs could give rise to ILC1s, ILC2s, and NKp46$^+$ ILC3s but not to conventional NK cells or CD4$^+$ LTi-like ILC3s. A model has been proposed whereby PLZF expression in ILCPs was associated with reduced generation of NK cells and CCR6$^+$ CD4$^+$ ILC3s. It was therefore of great interest to better understand the complexity of these different ILCP populations through analysis of Id2^{RFP}Zbtb16^{CreGFP} double-reporter mice. As expected (Constantinides et al., 2014), we found that *Id2*$^+$*Zbtb16*$^+$ ILCPs could robustly generate ILC1 and ILC2 subsets and showed strongly reduced potential for CCR6$^+$ ILC3s (LTi-like ILC3s). Moreover, we found that *Id2*$^+$*Zbtb16*$^+$ ILCPs gave rise to conventional NK cells both *in vitro* and *in vivo*, suggesting that these precursors retained substantial NK-cell-lineage potential. Generation of Eomes$^+$ NK-cell-containing clones was obtained from *Id2*$^+$*Zbtb16*$^+$ ILCPs, and these cells harbored Eomes-dependent cytotoxic molecules (perforin and granzyme B) after growth *in vitro*. Importantly, NK cells derived from *Id2*$^+$*Zbtb16*$^+$ ILCPs *in vivo* expressed markers of mature conventional NK cells (Ly49 receptors, CD49b) that were not expressed by ILC1s. These results indicate that PLZF expression in ILCPs is compatible with conventional NK-cell development, in contrast with the current models (Diefenbach et al., 2014; Constantinides et al., 2014). It is possible that NK-cell progeny from *Zbtb16*$^+$ ILCPs were not detected because Eomes staining was not performed in the previous study (Constantinides et al., 2014). The molecular mechanisms that promote NK-cell development from ILCPs remain unclear, although it is interesting to speculate that this process might be controlled in an analogous fashion to that which operates during intrathymic CD8-lineage determination (via cytokine-driven survival and expansion) (Cherrier et al., 2018).

By multiplexing *Id2*, *Zbtb16*, and *Bcl11b* reporters, we could confirm previous reports that identified early *Bcl11b* expression and ILC2 differentiation (Califano et al., 2015; Yu et al., 2015). The precise stage at which up-regulation of Bcl11b occurs to commit ILCPs to the ILC2 fate was not known. By studying Id2^{RFP}Zbtb16^{GFPcre}Bcl11b^{tdTomato} triple-reporter mice, we could demonstrate complexity in the ILCP compartment that raised additional questions concerning the progressive stages of ILC differentiation. We found that *Bcl11b* expression was enriched for ILC2 fate in *Id2*$^+$ ILCPs but that this process appeared independent of *Zbtb16* expression. A sequential model of ILC2 differentiation (*Zbtb16*$^+$*Bcl11b*$^-$ → *Zbtb16*$^+$*Bcl11b*$^+$ → *Zbtb16*$^-$*Bcl11b*$^+$) would accommodate the data and be consistent with previous fate-mapping studies (Constantinides et al., 2014), although *Zbtb16*-independent pathways may also exist. Further studies will be required to understand the inter-relationships between PLZF- and BCL11B-dependent ILC differentiation.

Analysis of Id2^{RFP}Zbtb16^{GFPcre}Bcl11b^{tdTomato} mice also demonstrated that in ILC3s, especially CCR6$^+$ ILC3s (LTi-like cells), differentiation was highly enriched in *Id2*$^+$*Zbtb16*$^-$*Bcl11b*$^-$ ILCPs. In contrast, expression of either *Zbtb16* or *Bcl11b* was associated with loss of ILC3 potential. As such, our results suggest that ILC3 emergence from *Id2*$^+$ ILCPs may represent one of the earliest branch points in ILC development, which separates ILC3 (via up-regulation of *Rorc*) from ILC1, ILC2, or NK-cell (via up-regulation of *Zbtb16*) pathways, which was also observed during fetal ILC differentiation (Ishizuka et al., 2016). Understanding the signals that instruct expression of these critical TFs should shed light on how these unique innate effector cells are generated and may lead to approaches that can promote their development in diverse disease settings.

STAR★METHODS

Detailed methods are provided in the online version of this paper and include the following:

- KEY RESOURCES TABLE
- CONTACT FOR REAGENT AND RESOURCE SHARING
- METHOD DETAILS
  - Mice
  - Cell Isolation
  - Flow Cytometric Analysis
  - Cell Culture
  - *In Vivo* Adoptive Transfer
  - Biomarker Analysis and qRT-PCR
- QUANTIFICATION AND STATISTICAL ANALYSIS

SUPPLEMENTAL INFORMATION

Supplemental Information can be found with this article online at https://doi.org/10.1016/j.immuni.2019.02.022.

ACKNOWLEDGMENTS

We thank Albert Bendelac for providing Zbtb16^{GFPCre} mice, Andreas Diefenbach for providing Id2^{GFP} mice, and Ana Cumano for providing OP9 and OP9-DL4 cells. We are grateful to Francina Langa-Vives and Franck Bourgade for their help with the generation of Id2^{RFP} mice and the CB-UTechS platform for cytometry support. We thank all the members of the Innate Immunity Unit for helpful discussions. D.E.C. is supported by the French Ministry of Higher Education, Research and Innovation. The Innate Immunity Unit is supported by grants from the Institut National de la Santé et de la Recherche Médicale (INSERM), Institut Pasteur, the Agence National pour le Recherche (ANR),

(C) Flow cytometry analysis of RORγt and CD27 expression on Id2^{RFP} ILCPs according to their expression of *Zbtb16* and *Bcl11b*. Data are from one experiment representative of two independent experiments.

(D) Flow cytometry analysis for mature ILCs after bulk culture of *Id2*$^+$*Zbtb16*$^-$*Bcl11b*$^-$, *Id2*$^+$*Zbtb16*$^+$*Bcl11b*$^-$, *Id2*$^+$*Zbtb16*$^+$*Bcl11b*$^+$, or *Id2*$^+$*Zbtb16*$^-$*Bcl11b*$^+$ ILCPs for 7 days on OP9 cells with SCF, IL-7, and IL-33. Data are from one experiment representative of three independent experiments.

(E) Percentage of mature ILC subsets among CD45$^+$ cells for (D).

(F) *In vitro* differentiation of single *Id2*$^+$*Zbtb16*$^-$*Bcl11b*$^-$, *Id2*$^+$*Zbtb16*$^+$*Bcl11b*$^-$, *Id2*$^+$*Zbtb16*$^+$*Bcl11b*$^+$, or *Id2*$^+$*Zbtb16*$^-$*Bcl11b*$^+$ ILCPs on OP9 cells. Cells were cultured during 15 days with SCF, IL-7, and IL-33. Please also see Figure S3.

and the European Research Council (ERC) under the European Union's Horizon 2020 research and innovation program (695467 – ILC_REACTIVITY).

AUTHOR CONTRIBUTIONS

W.X. and D.E.C. designed, performed, and analyzed experiments and wrote the manuscript; S.C. and M.P. analyzed the Biomark experiments; C.V. and R.G. helped edit the manuscript; N.S. performed experiments and helped prepare figures; P.L. provided Bcl11b^{tdTom} mice; and J.P.D. designed and directed the study and wrote the manuscript.

DECLARATION OF INTERESTS

The authors declare no competing interests.

Received: July 12, 2018
Revised: January 3, 2019
Accepted: February 25, 2019
Published: March 26, 2019

REFERENCES

Aliahmad, P., de la Torre, B., and Kaye, J. (2010). Shared dependence on the DNA-binding factor TOX for the development of lymphoid tissue-inducer cell and NK cell lineages. Nat. Immunol. *11*, 945–952.

Bando, J.K., Liang, H.E., and Locksley, R.M. (2015). Identification and distribution of developing innate lymphoid cells in the fetal mouse intestine. Nat. Immunol. *16*, 153–160.

Boos, M.D., Yokota, Y., Eberl, G., and Kee, B.L. (2007). Mature natural killer cell and lymphoid tissue-inducing cell development requires Id2-mediated suppression of E protein activity. J. Exp. Med. *204*, 1119–1130.

Califano, D., Cho, J.J., Uddin, M.N., Lorentsen, K.J., Yang, Q., Bhandoola, A., Li, H., and Avram, D. (2015). Transcription Factor Bcl11b Controls Identity and Function of Mature Type 2 Innate Lymphoid Cells. Immunity *43*, 354–368.

Carotta, S., Pang, S.H.M., Nutt, S.L., and Belz, G.T. (2011). Identification of the earliest NK-cell precursor in the mouse BM. Blood *117*, 5449–5452.

Chea, S., Possot, C., Perchet, T., Petit, M., Cumano, A., and Golub, R. (2015). CXCR6 Expression Is Important for Retention and Circulation of ILC Precursors. Mediators Inflamm. *2015*, 368427.

Cherrier, M., Sawa, S., and Eberl, G. (2012). Notch, Id2, and RORγt sequentially orchestrate the fetal development of lymphoid tissue inducer cells. J. Exp. Med. *209*, 729–740.

Cherrier, D., Serafini, N., and Di Santo, J.P. (2018). Innate Lymphoid Cell Development: A T Cell Perspective. Immunity *48*, 1091–1103.

Colucci, F., Soudais, C., Rosmaraki, E., Vanes, L., Tybulewicz, V.L., and Di Santo, J.P. (1999). Dissecting NK cell development using a novel alymphoid mouse model: investigating the role of the c-abl proto-oncogene in murine NK cell differentiation. J. Immunol. *162*, 2761–2765.

Constantinides, M.G., McDonald, B.D., Verhoef, P.A., and Bendelac, A. (2014). A committed precursor to innate lymphoid cells. Nature *508*, 397–401.

Constantinides, M.G., Gudjonson, H., McDonald, B.D., Ishizuka, I.E., Verhoef, P.A., Dinner, A.R., and Bendelac, A. (2015). PLZF expression maps the early stages of ILC1 lineage development. Proc. Natl. Acad. Sci. USA *112*, 5123–5128.

Cording, S., Medvedovic, J., Cherrier, M., and Eberl, G. (2014). Development and regulation of RORγt(+) innate lymphoid cells. FEBS Lett. *588*, 4176–4181.

Diefenbach, A., Colonna, M., and Koyasu, S. (2014). Development, differentiation, and diversity of innate lymphoid cells. Immunity *41*, 354–365.

Fathman, J.W., Bhattacharya, D., Inlay, M.A., Seita, J., Karsunky, H., and Weissman, I.L. (2011). Identification of the earliest natural killer cell-committed progenitor in murine bone marrow. Blood *118*, 5439–5447.

Hoshino, K., Tsutsui, H., Kawai, T., Takeda, K., Nakanishi, K., Takeda, Y., and Akira, S. (1999). Cutting edge: generation of IL-18 receptor-deficient mice: evidence for IL-1 receptor-related protein as an essential IL-18 binding receptor. J. Immunol. *162*, 5041–5044.

Hoyler, T., Klose, C.S.N., Souabni, A., Turqueti-Neves, A., Pfeifer, D., Rawlins, E.L., Voehringer, D., Busslinger, M., and Diefenbach, A. (2012). The transcription factor GATA-3 controls cell fate and maintenance of type 2 innate lymphoid cells. Immunity *37*, 634–648.

Ishizuka, I.E., Chea, S., Gudjonson, H., Constantinides, M.G., Dinner, A.R., Bendelac, A., and Golub, R. (2016). Single-cell analysis defines the divergence between the innate lymphoid cell lineage and lymphoid tissue-inducer cell lineage. Nat. Immunol. *17*, 269–276.

Jackson, J.T., Hu, Y., Liu, R., Masson, F., D'Amico, A., Carotta, S., Xin, A., Camilleri, M.J., Mount, A.M., Kallies, A., et al. (2011). Id2 expression delineates differential checkpoints in the genetic program of CD8α+ and CD103+ dendritic cell lineages. EMBO J. *30*, 2690–2704.

Kee, B.L. (2009). E and ID proteins branch out. Nat. Rev. Immunol. *9*, 175–184.

Klose, C.S.N., Flach, M., Möhle, L., Rogell, L., Hoyler, T., Ebert, K., Fabiunke, C., Pfeifer, D., Sexl, V., Fonseca-Pereira, D., et al. (2014). Differentiation of type 1 ILCs from a common progenitor to all helper-like innate lymphoid cell lineages. Cell *157*, 340–356.

Li, P., Burke, S., Wang, J., Chen, X., Ortiz, M., Lee, S.-C., Lu, D., Campos, L., Goulding, D., Ng, B.L., et al. (2010). Reprogramming of T cells to natural killer-like cells upon Bcl11b deletion. Science *329*, 85–89.

Lim, A.I., Li, Y., Lopez-Lastra, S., Stadhouders, R., Paul, F., Casrouge, A., Serafini, N., Puel, A., Bustamante, J., Surace, L., et al. (2017). Systemic Human ILC Precursors Provide a Substrate for Tissue ILC Differentiation. Cell *168*, 1086–1100.e10.

Monticelli, L.A., Buck, M.D., Flamar, A.-L., Saenz, S.A., Tait Wojno, E.D., Yudanin, N.A., Osborne, L.C., Hepworth, M.R., Tran, S.V., Rodewald, H.-R., et al. (2016). Arginase 1 is an innate lymphoid-cell-intrinsic metabolic checkpoint controlling type 2 inflammation. Nat. Immunol. *17*, 656–665.

Moro, K., Yamada, T., Tanabe, M., Takeuchi, T., Ikawa, T., Kawamoto, H., Furusawa, J., Ohtani, M., Fujii, H., and Koyasu, S. (2010). Innate production of T(H)2 cytokines by adipose tissue-associated c-Kit(+)Sca-1(+) lymphoid cells. Nature *463*, 540–544.

Nechanitzky, R., Akbas, D., Scherer, S., György, I., Hoyler, T., Ramamoorthy, S., Diefenbach, A., and Grosschedl, R. (2013). Transcription factor EBF1 is essential for the maintenance of B cell identity and prevention of alternative fates in committed cells. Nat. Immunol. *14*, 867–875.

Ohtsuka, T., Ishibashi, M., Gradwohl, G., Nakanishi, S., Guillemot, F., and Kageyama, R. (1999). Hes1 and Hes5 as notch effectors in mammalian neuronal differentiation. EMBO J. *18*, 2196–2207.

Possot, C., Schmutz, S., Chea, S., Boucontet, L., Louise, A., Cumano, A., and Golub, R. (2011). Notch signaling is necessary for adult, but not fetal, development of RORγt(+) innate lymphoid cells. Nat. Immunol. *12*, 949–958.

Ramirez, K., Chandler, K.J., Spaulding, C., Zandi, S., Sigvardsson, M., Graves, B.J., and Kee, B.L. (2012). Gene deregulation and chronic activation in natural killer cells deficient in the transcription factor ETS1. Immunity *36*, 921–932.

Rawlins, E.L., Clark, C.P., Xue, Y., and Hogan, B.L.M. (2009). The Id2+ distal tip lung epithelium contains individual multipotent embryonic progenitor cells. Development *136*, 3741–3745.

Rosmaraki, E.E., Douagi, I., Roth, C., Colucci, F., Cumano, A., and Di Santo, J.P. (2001). Identification of committed NK cell progenitors in adult murine bone marrow. Eur. J. Immunol. *31*, 1900–1909.

Satoh-Takayama, N., Lesjean-Pottier, S., Vieira, P., Sawa, S., Eberl, G., Vosshenrich, C.A.J., and Di Santo, J.P. (2010). IL-7 and IL-15 independently program the differentiation of intestinal CD3-NKp46+ cell subsets from Id2-dependent precursors. J. Exp. Med. *207*, 273–280.

Seehus, C.R., Aliahmad, P., de la Torre, B., Iliev, I.D., Spurka, L., Funari, V.A., and Kaye, J. (2015). The development of innate lymphoid cells requires TOX-dependent generation of a common innate lymphoid cell progenitor. Nat. Immunol. *16*, 599–608.

Seillet, C., Mielke, L.A., Amann-Zalcenstein, D.B., Su, S., Gao, J., Almeida, F.F., Shi, W., Ritchie, M.E., Naik, S.H., Huntington, N.D., et al. (2016). Deciphering the Innate Lymphoid Cell Transcriptional Program. Cell Rep. *17*, 436–447.

Serafini, N., Klein Wolterink, R.G.J., Satoh-Takayama, N., Xu, W., Vosshenrich, C.A.J., Hendriks, R.W., and Di Santo, J.P. (2014). Gata3 drives development of RORγt+ group 3 innate lymphoid cells. J. Exp. Med. *211*, 199–208.

Serafini, N., Vosshenrich, C.A., and Di Santo, J.P. (2015). Transcriptional regulation of innate lymphoid cell fate. Nat. Rev. Immunol. *15*, 415–428.

Suzuki, H., Duncan, G.S., Takimoto, H., and Mak, T.W. (1997). Abnormal development of intestinal intraepithelial lymphocytes and peripheral natural killer cells in mice lacking the IL-2 receptor beta chain. J. Exp. Med. *185*, 499–505.

Vivier, E., Artis, D., Colonna, M., Diefenbach, A., Di Santo, J.P., Eberl, G., Koyasu, S., Locksley, R.M., McKenzie, A.N.J., Mebius, R.E., et al. (2018). Innate Lymphoid Cells: 10 Years On. Cell *174*, 1054–1066.

Wong, S.H., Walker, J.A., Jolin, H.E., Drynan, L.F., Hams, E., Camelo, A., Barlow, J.L., Neill, D.R., Panova, V., Koch, U., et al. (2012). Transcription factor RORα is critical for nuocyte development. Nat. Immunol. *13*, 229–236.

Xu, W., Domingues, R.G.G., Fonseca-Pereira, D., Ferreira, M., Ribeiro, H., Lopez-Lastra, S., Motomura, Y., Moreira-Santos, L., Bihl, F., Braud, V., et al. (2015). NFIL3 orchestrates the emergence of common helper innate lymphoid cell precursors. Cell Rep. *10*, 2043–2054.

Yang, Q., and Bhandoola, A. (2016). The development of adult innate lymphoid cells. Curr. Opin. Immunol. *39*, 114–120.

Yang, C.Y., Best, J.A., Knell, J., Yang, E., Sheridan, A.D., Jesionek, A.K., Li, H.S., Rivera, R.R., Lind, K.C., D'Cruz, L.M., et al. (2011). The transcriptional regulators Id2 and Id3 control the formation of distinct memory CD8+ T cell subsets. Nat. Immunol. *12*, 1221–1229.

Yang, Q., Li, F., Harly, C., Xing, S., Ye, L., Xia, X., Wang, H., Wang, X., Yu, S., Zhou, X., et al. (2015). TCF-1 upregulation identifies early innate lymphoid progenitors in the bone marrow. Nat. Immunol. *16*, 1044–1050.

Yokota, Y., Mansouri, A., Mori, S., Sugawara, S., Adachi, S., Nishikawa, S., and Gruss, P. (1999). Development of peripheral lymphoid organs and natural killer cells depends on the helix-loop-helix inhibitor Id2. Nature *397*, 702–706.

Yoshida, H., Kawamoto, H., Santee, S.M., Hashi, H., Honda, K., Nishikawa, S., Ware, C.F., Katsura, Y., and Nishikawa, S.-I. (2001). Expression of alpha(4) beta(7) integrin defines a distinct pathway of lymphoid progenitors committed to T cells, fetal intestinal lymphotoxin producer, NK, and dendritic cells. J. Immunol. *167*, 2511–2521.

Yu, X., Wang, Y., Deng, M., Li, Y., Ruhn, K.A., Zhang, C.C., and Hooper, L.V. (2014). The basic leucine zipper transcription factor NFIL3 directs the development of a common innate lymphoid cell precursor. eLife *3*, 945–952.

Yu, Y., Wang, C., Clare, S., Wang, J., Lee, S.C., Brandt, C., Burke, S., Lu, L., He, D., Jenkins, N.A., et al. (2015). The transcription factor Bcl11b is specifically expressed in group 2 innate lymphoid cells and is essential for their development. J. Exp. Med. *212*, 865–874.

Yu, Y., Tsang, J.C.H.H., Wang, C., Clare, S., Wang, J., Chen, X., Brandt, C., Kane, L., Campos, L.S., Lu, L., et al. (2016). Single-cell RNA-seq identifies a PD-1^{hi} ILC progenitor and defines its development pathway. Nature *539*, 102–106.

Zook, E.C., and Kee, B.L. (2016). Development of innate lymphoid cells. Nat. Immunol. *17*, 775–782.

Zook, E.C., Ramirez, K., Guo, X., van der Voort, G., Sigvardsson, M., Svensson, E.C., Fu, Y.X., and Kee, B.L. (2016). The ETS1 transcription factor is required for the development and cytokine-induced expansion of ILC2. J. Exp. Med. *213*, 687–696.

STAR★METHODS

KEY RESOURCES TABLE

REAGENT or RESOURCE	SOURCE	IDENTIFIER
Antibodies		
Anti-mouse CD3	BioLegend	Cat# 100241; RRID: AB_2563945
Anti-mouse CD19	BD Biosciences	Cat# 563333; RRID: AB_2738141
Anti-mouse NKp46	eBiosciences	Cat# 12-3351-82; RRID: AB_1210743
Anti-mouse NK1.1	BioLegend	Cat# 108724; RRID: AB_830871
Anti-mouse CD49a	BD Biosciences	Cat# 562115; RRID: AB_11153117
Anti-mouse CD49b	BioLegend	Cat# 108912; RRID: AB_492880
Anti-mouse CD4	BD Biosciences	Cat# 553047; RRID: AB_394583
Anti-mouse ICOS	BioLegend	Cat# 313524; RRID: AB_2562545
Anti-mouse T1/ST2	BD Biosciences	Cat# 566312; RRID: AB_2744490
Anti-mouse CD90	BD Biosciences	Cat# 564365; RRID: AB_2734760
Anti-mouse CD127	eBiosciences	Cat# 25-1271-82; RRID: AB_469649
Anti-mouse CD25	eBiosciences	Cat# 12-0251-82; RRID: AB_465607
Anti-mouse CD27	BD Biosciences	Cat# 561245; RRID: AB_10611853
Anti-mouse CD244	BD Biosciences	Cat# 553306; RRID: AB_394770
Anti-mouse CD117	BD Biosciences	Cat# 563160; RRID: AB_2722510
Anti-mouse Sca1	eBiosciences	Cat# 56-5981-82; RRID: AB_657836
Anti-mouse CD135	eBiosciences	Cat# 46-1351-82; RRID: AB_10733393
Anti-mouse CD122	eBiosciences	Cat# 48-1222-82; RRID: AB_2016697
Anti-mouse α4β7	eBiosciences	Cat# 17-5887-80; RRID: AB_1210578
Anti-mouse KLRG1	eBiosciences	Cat# 17-5893-82; RRID: AB_469469
Anti-mouse Ly49G2	eBiosciences	Cat# 46-5781-82; RRID: AB_1834437
Anti-human/mouse GATA3	eBiosciences	Cat# 46-9966-42; RRID: AB_10804487
Anti-mouse PLZF	BD Biosciences	Cat# 563490; RRID: AB_2738238
Anti-mouse PD1	BioLegend	Cat# 135223; RRID: AB_2563522
Anti-mouse Perforin	eBiosciences	Cat# 12-9392-82; RRID: AB_466243
Anti-human/mouse Granzyme	BioLegend	Cat# 515408; RRID: AB_2562196
Anti-mouse RORgt	BD Biosciences	Cat# 562684; RRID: AB_2651150
Anti-mouse CCR6	BioLegend	Cat# 129819; RRID: AB_2562513
Anti-mouse EOMES	eBiosciences	Cat# 50-4875-82; RRID: AB_2574227
Anti-mouse TBET	eBiosciences	Cat# 25-5825-82; RRID: AB_11042699
Anti-mouse IFNg	BD Biosciences	Cat# 557724; RRID: AB_396832
Anti-mouse IL-5	eBiosciences	Cat# 12-7052-82; RRID: AB_763587
Anti-mouse IL-22	eBiosciences	Cat# 12-7221-82; RRID: AB_10597428
FcR Blocking Reagent, mouse	Miltenyi Biotec	Cat# 130-092-575
Chemicals, Peptides, and Recombinant Proteins		
Streptavidin	BD Biosciences	Cat# 554063
Fixable viability dye	eBiosciences	Cat# 65-0866-18
Anti-Biotin MicroBeads UltraPure	Miltenyi Biotec	Cat# 130-105-637
Percoll	GE Healthcare	Cat# 17-0891-01
Liberase TL Research Grade	Roche	Cat# 05401020001
DNAse I	Roche	Cat# 10104159001
Penicillin-Streptomycin (5,000 U/mL)	Thermo Fischer	Cat# 15070-063
2-Mercaptoethanol	Thermo Fischer	Cat# 31350-010

(*Continued on next page*)

Continued

REAGENT or RESOURCE	SOURCE	IDENTIFIER
Opti-MEM Reduced Serum Medium, GlutaMAX Supplement	Thermo Fischer	Cat# 51985034
Mouse IL-7, research grade	Miltenyi Biotec	Cat# 130-094-066
Mouse IL-33, research grade	Miltenyi Biotec	Cat# 130-112-961
Mouse SCF, premium grade	Miltenyi Biotec	Cat# 130-101-693
Mouse IL-23, research grade	Miltenyi Biotec	Cat# 130-096-676
Mouse IL-2, research grade	Miltenyi Biotec	Cat# 130-094-055
Experimental Models: Cell Lines		
Mouse: OP9	Institut Pasteur	Cat# CRL-2749
Mouse: OP9-DL4	Institut Pasteur	N/A
Experimental Models: Organisms/Strains		
Mouse: Zbtb16GFPcre	U. Chicago	Constantinides et al., 2014
Mouse: Bcl11btdTomato	Sanger Institute	Li et al., 2010
Mouse: Rag2$^{-/-}$ Il2rg$^{-/-}$	Institut Pasteur	Colucci et al., 1999
Mouse: Id2RFP	Institut Pasteur	N/A
Mouse: C57BL6/J	Institut Pasteur	N/A
Mouse: Id2GFP	Charité Berlin	Rawlins et al., 2009
Oligonucleotides		
Taqman gene primers for Biomark analysis	This paper	See Table S1
Software and Algorithms		
Flow Jo_v10	FlowJo	https://www.flowjo.com/
Prism 7	Prism-Graphpad	https://www.graphpad.com

CONTACT FOR REAGENT AND RESOURCE SHARING

Further information and requests for resources and reagents should be directed to and will be fulfilled by the Lead Contact, James Di Santo (james.di-santo@pasteur.fr).

METHOD DETAILS

Mice

Mice were bred in dedicated facilities of the Institut Pasteur. Id2^{RFP} mice were generated by genOway (Lyon, FR) by insertion of an IRES-mRFP cassette downstream of the STOP codon in 3′ UTR region of *Id2* exon 2 using homologous recombination in C57BL/6 ESCs. Correctly targeted ESCs were microinjected into Balb/c blastocysts to generate chimeric mice and germline transmission was verified after breeding with C57BL/6 females. Zbtb16^{GFPcre} (Constantinides et al., 2014), Bcl11b^{tdTomato} (Li et al., 2010), Id2^{GFP} (Rawlins et al., 2009) and *Rag2*$^{-/-}$*Il2rg*$^{-/-}$ mice (Colucci et al., 1999) were on the C57BL/6 background. Procedures involving mice were previously approved by local Animal Ethics Committees and registered with the French authorities.

Cell Isolation

Lymphocyte preparations from spleen and LNs were prepared using 70 μm strainers. BM cells were collected by either flushing or crushing bones. Lungs were minced and incubated 30 min at 37oC with agitation in HBSS with 5mM EDTA, 10mM HEPES and 5% FBS followed by 1 hr digestion with collagenase D (5 mg/ml; Roche) and DNase I (0.1 mg/ml; Roche) in RPMI, 5% FBS with 10 mM HEPES. Sequentially cells were purified by centrifugation 30 min at 2400 rpm in 40/80 Percoll (Sigma) gradient. Small intestines were cut, washed with PBS 1 × 5 mM EDTA 15 min at 37oC with agitation. IELs were removed using a 100 μm cell strainer, the remaining pieces were digested 30 min at 37oC with agitation in RPMI with 10 mM HEPES and 5% FBS, collagenase D (5mg/ml; Roche) and DNase I (0.1 mg/ml; Roche). Sequentially cells were purified by centrifugation 30 min at 2400 rpm in 40/80 Percoll gradient. Livers were smashed and cells were purified by centrifugation 30 min at 2400 rpm in 35% Percoll.

Flow Cytometric Analysis

Cells were stained for surface markers for 30 min at 4°C, except for CCR6 (37°C for 15 min then at 4°C for 15 min). Transcription factors were analyzed after cell fixation in either 4% PFA in PBS (20 min at 4°C) or using a commercial fixative according to manufacturer's instructions (eBioscience). Antibodies used in this study are listed in the Key Resources Table. Labeled cells were analyzed using a Fortessa flow cytometer (BD Biosciences) or sorted using a FACSAria III. The data were analyzed with FlowJo software.

Cell Culture

Cells were cultured using flat-bottom 96-well plates previously coated with 1000 OP9 or OP9-DL4 stromal cells in 10% FCS, 50 U penicillin (Invitrogen), 50 mg/mL streptomycin (Invitrogen), 50 mM β-mercaptoethanol (Invitrogen). Stem Cell Factor (20 ng/mL), IL-7 (20 ng/mL), IL-33 (10 ng/mL), IL-23 (10 ng/mL), IL-2 (10 ng/mL), IL-15 (10 ng/mL) or IL-12 (10 ng/mL) were added in the medium when specified. Half of the medium was removed and replaced by fresh medium every 3 days. Visible clones were analyzed by flow cytometry after 10-14 days.

In Vivo Adoptive Transfer

After dissection of femur, tibia, and pelvis, the bones were crushed, and cell suspensions were filtered through 100uM sieves before red cell depletion. Lin^+ cells were depleted using biotin-coupled antibodies and anti-Biotin MicroBeads (Miltenyi Biotec), in accordance with the manufacturer's indications. Lineage cocktail included TCRβ, TCRγδ, CD3ε, CD8, CD19, B220, NK1.1, CD11b, CD11c, Gr-1, CD115 and Ter119 (for clone details, see Table S3). Sorted lymphoid progenitors (CLP, ILCP subsets) were retro-orbitally injected into sub-lethally irradiated 5-week-old *Rag2*$^{-/-}$*Il2rg*$^{-/-}$ mice. 800 ILCPs (unfractionated *Id2*$^+$, *Id2*$^+$*Zbtb16*$^+$, *Id2*$^{+-}$ *Zbtb16*$^-$) or 2000 CLP were injected into each recipient. After 5 weeks, recipient mice were sacrificed and organs were collected for analysis.

Biomarker Analysis and qRT-PCR

For Biomark analysis, cells were sorted in 96-well qPCR plates in 10 μl of the Cells Direct One-Step qRT-PCR Kit (Thermo Fisher Scientific), containing a mix of diluted primers (0.05× final concentration; see Table S1). Pre-amplified cDNA was obtained after reverse transcription and pre-amplification, and was diluted 1:5 in TE Buffer, pH 8 (Ambion). Sample mix was prepared as follows: diluted cDNA (2.9 μl), Sample Loading Reagent (0.29 μl, Fluidigm), TaqMan Universal PCR Master Mix (3.3 μl, Applied Biosystems). Assay mix was as follows: Assay Loading Reagent (2.5 μl, Fluidigm), TaqMan (2.5 μl, Applied Biosystems). A 48.48 dynamic array integrated fluidic circuit (IFC; Fluidigm) was primed with control line fluid, and the chip was loaded with assays (TaqMan) and samples using an HX IFC controller (Fluidigm). The experiments were run on a Biomark HD (Fluidigm) for amplification and detection (2′ at 50°C, 10′ at 95°C, 40 cycles: 15′′ at 95°C, 60′′ at 60°C). Heatmaps of two-dimensional hierarchical clustering analysis were performed by Qlucore Omics Explorer software. For qRT-PCR, cells were sorted in RLT Buffer (QIAGEN), RNA was obtained with the RNeasy Micro Kit (QIAGEN), and cDNA was obtained using SuperScript III Reverse Transcriptase (Invitrogen). A 7300 Real-Time PCR System (Applied Biosystems) and Solaris primers (GE Dharmacon) were used.

QUANTIFICATION AND STATISTICAL ANALYSIS

Statistic tests were performed using Prism software. Variance equality was tested using an F-test. Samples were there analyzed using Student's t tests or Mann-Whitney U tests (for samples that did not follow a normal distribution) as indicated.

Immunity, Volume *50*

Supplemental Information

An Id2^{RFP}-Reporter Mouse Redefines Innate Lymphoid Cell Precursor Potentials

Wei Xu, Dylan E. Cherrier, Sylvestre Chea, Christian Vosshenrich, Nicolas Serafini, Maxime Petit, Pentao Liu, Rachel Golub, and James P. Di Santo

Supplemental Figures and Tables

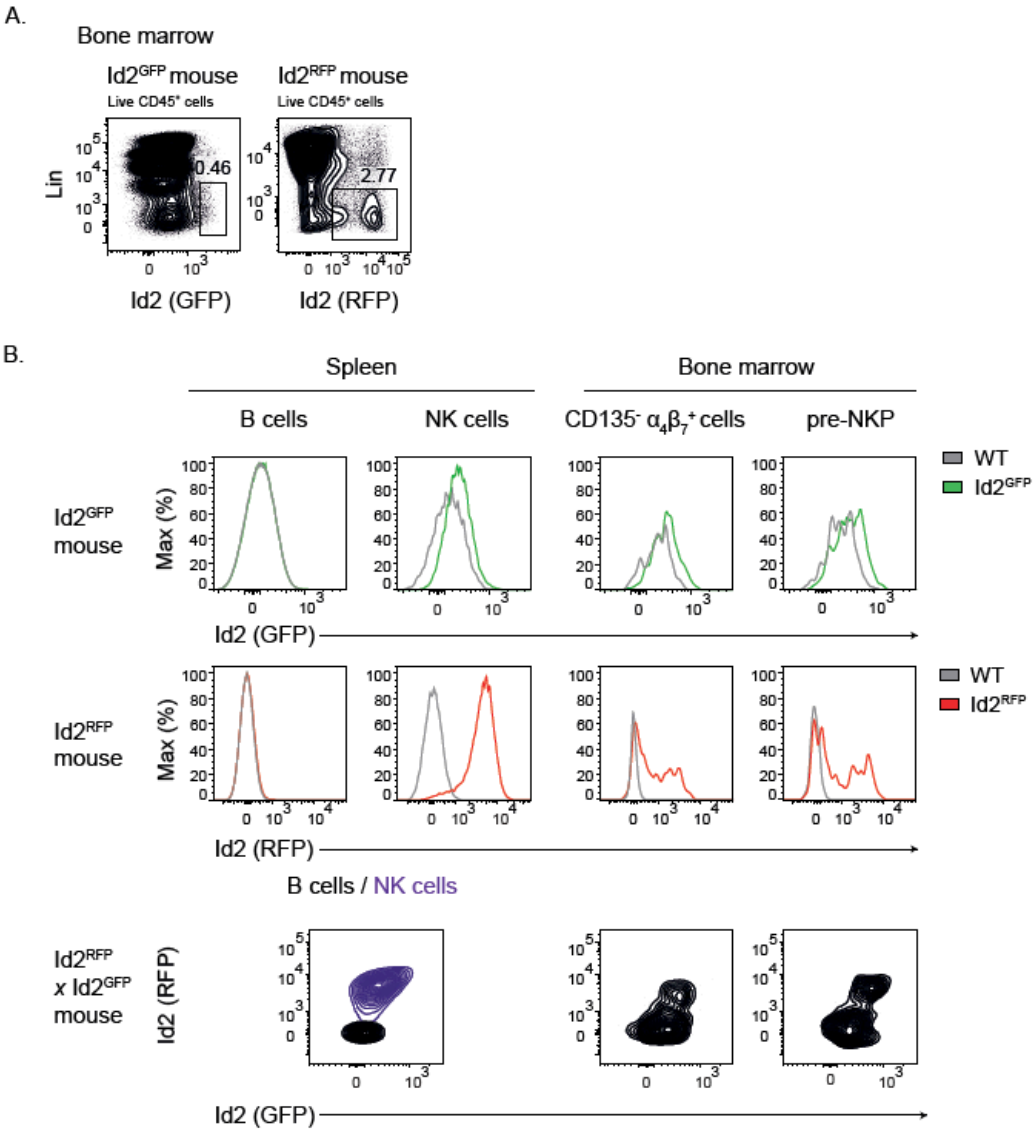

Figure S1. **Comparison of Id2^{GPF} and Id2^{RFP} mice, related to Figures 1, 2.** (A) Representative FACS plots of GFP and RFP expression in total bone marrow. (B) GFP and RFP expression in splenic B and NK cells, and in bone marrow CD135$^{-}\alpha_4\beta_7^{+}$ cells and pre-NKP in Id2^{GPF}, Id2^{RFP} and Id2^{RFP} x Id2^{GFP} mice.

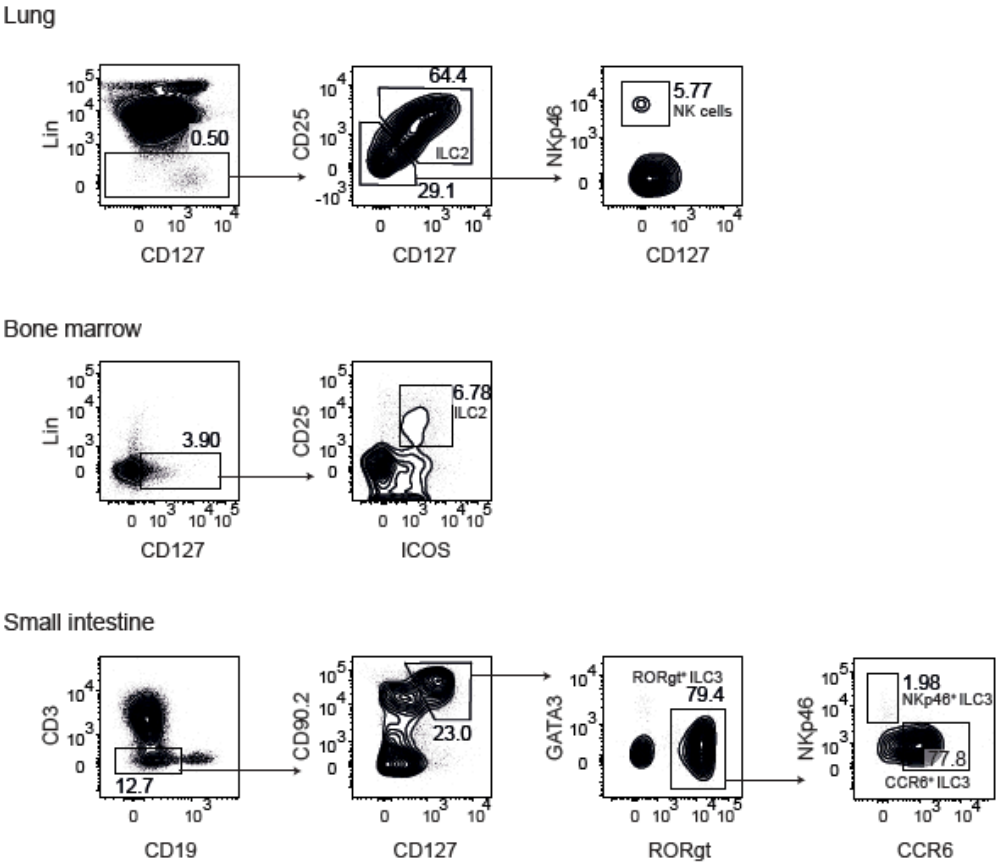

Figure S2. **ILC gating strategy for tissues, related to Figure 3.**

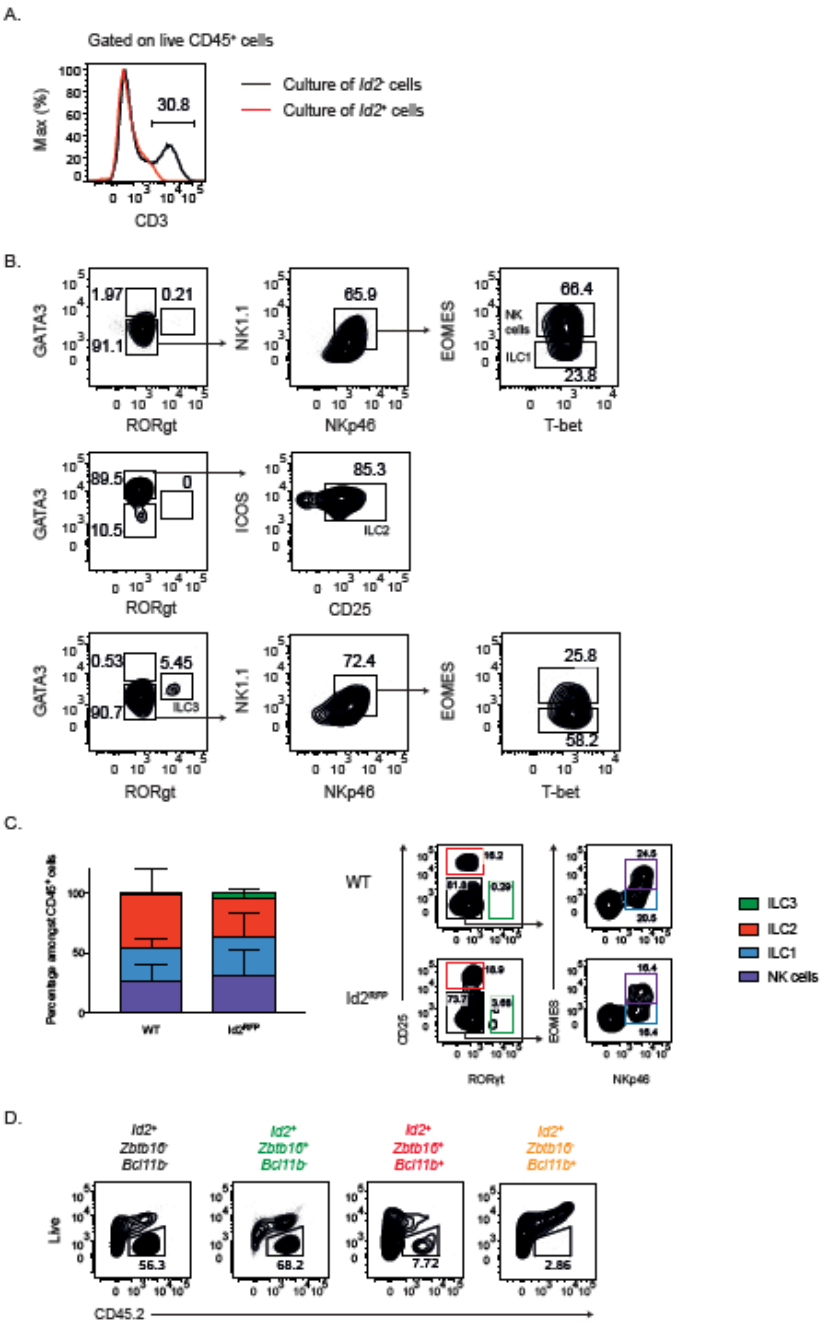

Figure S3. **Bone marrow precursors potential *in vitro*, related to Figure 3.** (A) CD3 expression on bulk cultured Lin$^-$CD127$^+$CD25$^-$ICOS$^-$CD117$^+$CD135$^-$$\alpha_4\beta_7^+$*Id2*$^-$ or *Id2*$^+$ cells on OP9-DL4 stroma and supplemented with SCF and IL-7 for 7 days. (B) Gating strategy for analysis of Id2$^+$ ILCP clonal cultures. (C) Analysis of bulk cultured Lin$^-$CD127$^+$CD25$^-$ICOS$^-$CD117$^+$CD135$^-$$\alpha_4\beta_7^+$ cells on OP9 stroma supplemented with SCF and IL-7 from WT or Id2^{RFP} mice (n=4; error bars represent standard error of the mean) with associated representative FACS plots. (D) Bulk culture of Id2 Zbtb16 Bcl11b ILCP subsets on OP9 stroma and supplemented with SCF and IL-7.

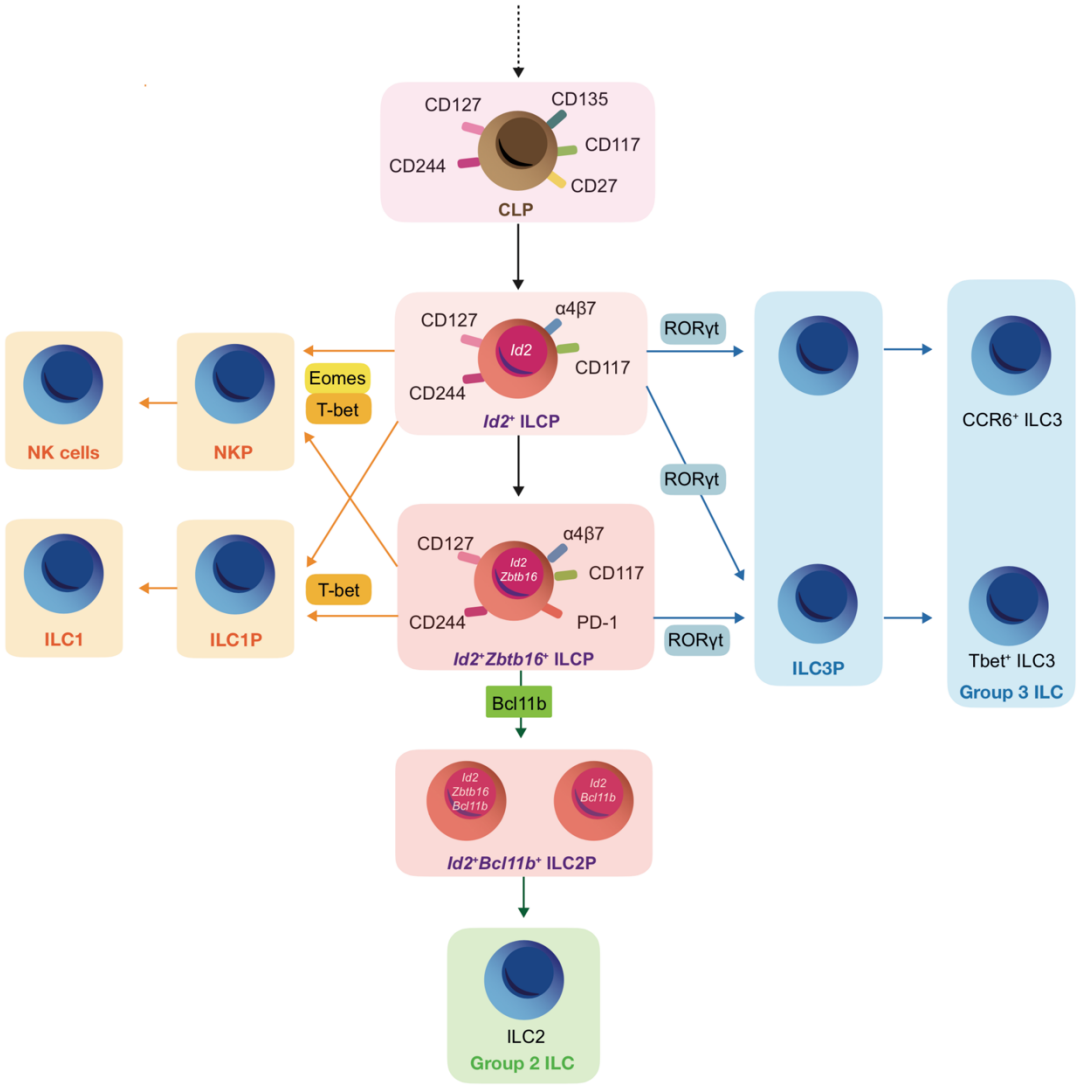

Figure S4. **Model for ILC development, related to Figure 7.**

Table S1. **Taqman gene primers used for Biomark analysis, related to STAR Methods.**

Gene	Ref	Gene	Ref
Actb	Mm00607939_s1	*Il2ra*	Mm01340213_m1
Ahr	Mm00478932_m1	*Il2rb*	Mm01195267_m1
Arg1	Mm00475988_m1	*Il7r*	Mm00434295_m1
Bcl11a	Mm00479358_m1	*Il17rb*	Mm00444709_m1
Bcl11b	Mm00480516_m1	*Il18r1*	Mm00515178_m1
Bcl2	Mm00477631_m1	*Itga4*	Mm00439770_m1
Bmpr2	Mm00432134_m1	*Nfil3*	Mm00600292_s1
CD27	Mm01185212_g1	*Notch1*	Mm00435249_m1
Cxcr5	Mm00432086_m1	*Notch2*	Mm00803069_m1
Cxcr6	Mm02620517_s1	*Rag2*	Mm00501300_m1
Dtx1	Mm00492297_m1	*Rora*	Mm01173766_m1
Ebf1	Mm00395519_m1	*Rorc*	Mm01261022_m1
Eomes	Mm01351985_m1	*Runx1*	Mm01213405_m1
Ets1	Mm01175819_m1	*Runx3*	Mm00450960_m1
Ets2	Mm00468977_m1	*Tbx21*	Mm00493445_m1
Gapdh	Mm03302249_g1	*Tcf7*	Mm01173766_m1
Gata3	Mm00484683_m1	*Tcf12*	Mm00441699_m1
Gfi1	Mm00515855_m1	*Tgfbr2*	Mm00436977_m1
Hes1	Mm01342805_m1	*Tox*	Mm00455231_m1
Hprt	Mm00446968_m1	*Zbtb7b*	Mm01176868_m1
Icos	Mm00497600_m1	*Zbtb16*	Mm00784709_s1
Id2	Mm00711781_m1		
Il1r1	Mm00434237_m1		
Il1rl1	Mm00516117_m1		

Table S2. **Frequency of clones containing NK, ILC1, ILC2 or ILC3 generated from A) Id2^{+} ILCP or B) Id2^{+}PLZF^{+} ILCP, related to Figures 3 and 5.**

A.

%	*Id2*$^{+}$ ILCP					
	OP9 cells		OP9-DL4 cells			
	SCF / IL-7		SCF / IL-7 / IL-33		SCF / IL-7 / IL-33 / IL-2 / IL-23	
NK vs. non-NK	82,76	17,24	73,86	26,14	85,20	14,80
ILC1 vs. non-ILC1	3,45	96,55	56,86	43,14	27,19	72,81
ILC2 vs. non-ILC2	10,34	89,66	26,14	73,86	29,00	71,00
ILC3 vs. non-ILC3	13,79	86,21	14,38	85,62	6,65	93,35

B.

%	*Id2*$^{+}$ *Zbtb16*$^{+}$ ILCP					
	OP9 cells		OP9-DL4 cells			
	SCF / IL-7		SCF / IL-7 / IL-33		SCF / IL-7 / IL-33 / IL-2 / IL-23	
NK vs. non-NK	90,00	10,00	47,06	52,94	82,14	17,86
ILC1 vs. non-ILC1	30,00	70,00	61,76	38,24	8,93	91,07
ILC2 vs. non-ILC2	6,67	93,33	52,94	47,06	25,60	74,40
ILC3 vs. non-ILC3	0,00	100,00	11,76	88,24	0,00	100,00